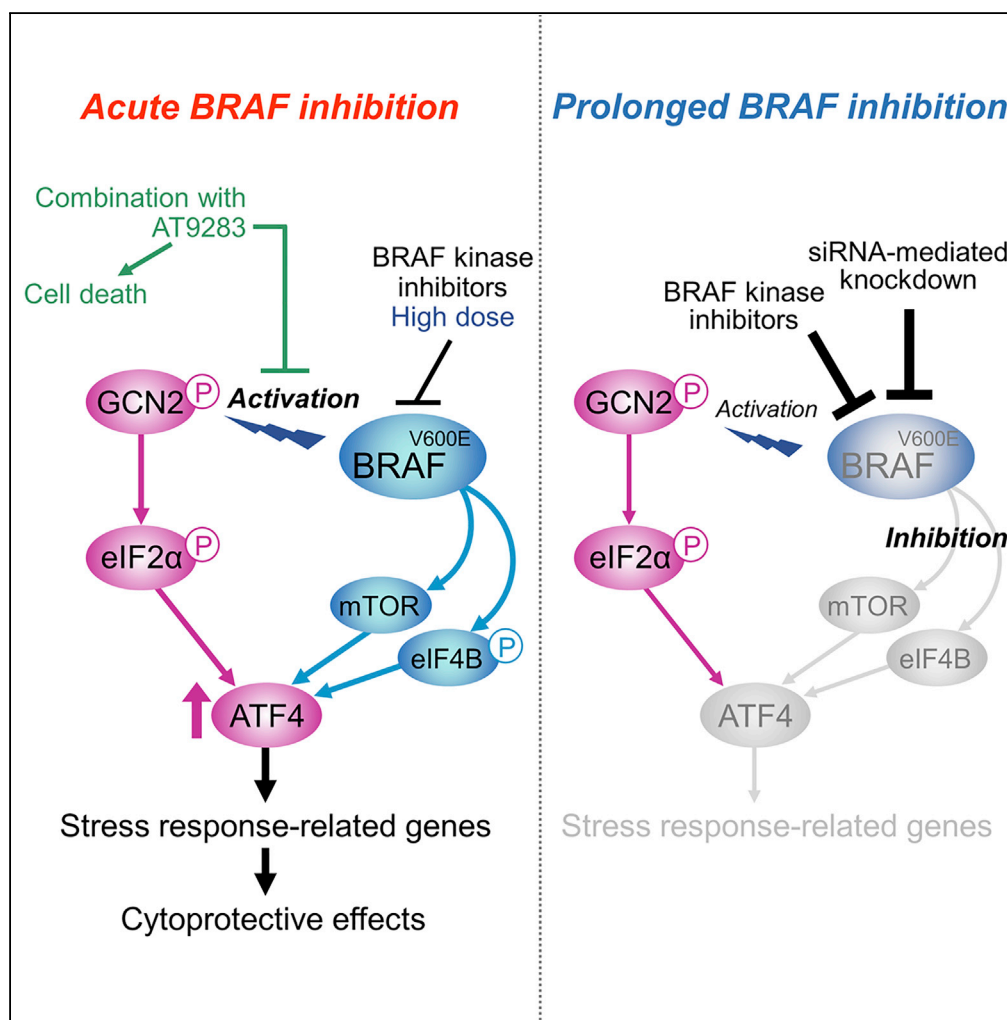**Article**

Disrupting ATF4 Expression Mechanisms Provides an Effective Strategy for BRAF-Targeted Melanoma Therapy

Ikuko Nagasawa,
Masaru Koido,
Yuri Tani, Satomi
Tsukahara,
Kazuhiro
Kunimasa, Akihiro
Tomida

akihiro.tomida@jfcr.or.jp

HIGHLIGHTS

Oncogenic BRAF signals mTOR and eIF4B to ensure ATF4 induction under GCN2 activation

The signaling pathway decays relatively slowly during BRAF kinase inhibition

The slow signaling decay enables adaptive response via the GCN2-ATF4 pathway

The GCN2-ATF4 activation mechanisms by BRAF inhibitors may provide druggable targets

DATA AND CODE AVAILABILITY
GSE136615

Article

Disrupting ATF4 Expression Mechanisms Provides an Effective Strategy for BRAF-Targeted Melanoma Therapy

Ikuko Nagasawa,[1] Masaru Koido,[1] Yuri Tani,[1] Satomi Tsukahara,[1] Kazuhiro Kunimasa,[1] and Akihiro Tomida[1,2,*]

SUMMARY

BRAF V600 **mutation influences cellular signaling pathways for melanoma development. However, the role of oncogenic BRAF in adaptive stress response pathways is not fully understood. Here, we show that oncogenic BRAF plays an essential role in the induction of ATF4 following the activation of general control non-derepressible 2 (GCN2) kinase during nutrient stress and BRAF-targeted, therapeutic stress. Under GCN2 activation, BRAF ensures ATF4 induction by utilizing mTOR and eIF4B as downstream regulators. In contrast to the MEK-ERK pathway, this signaling pathway remains temporarily active even during treatment with BRAF inhibitors, thereby enabling the transient induction of ATF4. We also identify a chemical compound that prevents BRAF inhibitor-induced activation of the GCN2-ATF4 pathway and produces synergistic cell killing with BRAF inhibitors. Our findings establish a collaborative relationship between oncogenic BRAF and the GCN2-ATF4 signaling pathway, which may provide a novel therapeutic approach to target the adaptive stress response.**

INTRODUCTION

Oncogenic mutations of *BRAF* are observed in approximately 50% of patients with melanoma (Schadendorf et al., 2018). The most common mutation is the substitution of valine at position 600 by glutamic acid (V600E), which results in constitutive activation of its kinase activity, leading to tumor initiation, progression, metastasis, and therapy resistance (Schadendorf et al., 2018). Mechanistically, the mutationally activated BRAF directly induces hyperactivation of the downstream MEK-ERK pathway (Davies et al., 2002) and also acts in cooperation with other genetic abnormalities, such as loss of function of *PTEN*, a negative regulator of the PI3K-Akt-mTOR pathway (The Cancer Genome Atlas Network, 2015). BRAF has also been reported to promote immune suppression (Bradley et al., 2016; Shabaneh et al., 2018). Thus, BRAF mutation can widely influence cellular signaling pathways and functions in the development of malignant melanoma.

BRAF inhibitors and the combination of BRAF and MEK inhibitors have shown impressive clinical efficacy in patients with BRAF-mutated melanoma (Chapman et al., 2011; Robert et al., 2015), but drug resistance generally remains inevitable. Resistant tumors frequently arise due to reactivation of the MEK-ERK pathway through multiple mechanisms, including amplification of *BRAF*, splice site mutations in *BRAF*, *de novo* mutations in *NRAS* or *MEK*, or upregulation of receptor tyrosine kinases (Das Thakur and Stuart, 2014; Van Allen et al., 2014). Drug resistance is also associated with non-mutational drug-tolerant states of cells, seen at the early phase of treatments (Raha et al., 2014; Sharma et al., 2010). Indeed, BRAF inhibitors, immediately after their administration to drug-sensitive cells, lead to reactivation of the MEK-ERK pathway (Hatzivassiliou et al., 2010) and metabolic reprogramming similar to that seen in drug-resistant cells (Parmenter et al., 2014). Thus, along with acquired vulnerability of drug-resistant cells (Hangauer et al., 2017; Wang et al., 2018), understanding the early response of drug-sensitive cells to BRAF inhibitors can provide clues to circumvent resistance and maximize the therapeutic efficacy.

To cope with diverse stresses, including environmental and therapeutic stresses, cancer cells often activate the integrated stress response (ISR) pathway, which is initiated by activation of eukaryotic initiation factor 2α (eIF2α) kinases (Pakos-Zebrucka et al., 2016). There are four different eIF2α kinases: general control non-derepressible 2 (GCN2), protein kinase-like endoplasmic reticulum (ER) kinase (PERK), protein kinase double-stranded RNA-dependent (PKR), and heme-regulated inhibitor (HRI), which sense distinct types of stress, typically, amino acid limitation, ER stress, viral infection, and heme deficiency, respectively (Pakos-Zebrucka et al., 2016). These eIF2α kinases catalyze the phosphorylation of eIF2α on serine 51, which

[1]Cancer Chemotherapy Center, Japanese Foundation for Cancer Research, Tokyo 135-8550, Japan

[2]Lead Contact

*Correspondence: akihiro.tomida@jfcr.or.jp

https://doi.org/10.1016/j.isci. 2020.101028

attenuates general protein synthesis while promoting the translation of *ATF4* mRNA with upstream open reading frames that enable preferential translation (Vattem and Wek, 2004). ATF4 is a key ISR transcription factor that induces the expression of genes involved in stress adaptation, such as amino acid and redox metabolism (Pakos-Zebrucka et al., 2016).

We previously demonstrated that the BRAF kinase inhibitors vemurafenib (10 μM) and dabrafenib (1 μM), at relatively high but clinically relevant concentrations (Falchook et al., 2014; Flaherty et al., 2010), can rapidly induce ATF4 in melanoma cells with BRAF^{V600E} mutation (Nagasawa et al., 2017). As the silencing of *ATF4* expression sensitizes cells to vemurafenib, this rapid induction of ATF4 can contribute to cell survival during treatments with BRAF inhibitors. Mechanistically, this ATF4 induction occurs via the GCN2 arm of the ISR, which is primarily activated in response to amino acid limitation. This observation, together with previous findings that metabolic reprogramming toward glutamine addiction occurred with the acquisition of resistance by chronic exposure to BRAF inhibitors (Baenke et al., 2016; Hernandez-Davies et al., 2015), suggests that modulating the metabolism of amino acids, especially glutamine, through ATF4 induction may be important for early adaptation to BRAF inhibition. However, the role of oncogenic BRAF in the adaptive mechanisms inducing ATF4 is not well understood.

We show herein that oncogenic BRAF exerts activity to drive the expression of ATF4 and can be associated with ATF4 target gene expression in patients with melanoma. In contrast to the MEK-ERK pathway, this signaling pathway that utilizes mTOR and eIF4B as downstream regulators for ATF4 expression remains temporarily active even during exposure to BRAF inhibitors, leading to ATF4 induction in cooperation with the GCN2 arm of the ISR pathway. We also identify a small compound that prevents the activation of the GCN2-ATF4 pathway and synergistically kills melanoma cells during BRAF inhibitor treatments. Our results demonstrate that BRAF-driven ATF4 expression mechanisms can provide a new strategy to circumvent resistance to BRAF-targeted therapy.

RESULTS

BRAF Kinase Inhibitors Induce ATF4 Expression Transiently

Treatments with BRAF kinase inhibitors, 10 μM vemurafenib as well as 1 μM dabrafenib, for 4 h clearly induced GCN2 phosphorylation, eIF2α phosphorylation, and ATF4 expression in BRAF-mutated A375 and G-361 cells (Figures 1A and S1A), as we previously reported (Nagasawa et al., 2017). Activation of the GCN2-ATF4 pathway was also seen upon 4 h of treatment with PLX7904 (Figure 1B), a different type of BRAF kinase inhibitor that has overcome the paradoxical property of vemurafenib and dabrafenib for ERK signaling (Zhang et al., 2015). Thus, ATF4 induction through GCN2 activation appears to be a common feature of BRAF kinase inhibitors. However, the increases in ATF4 expression levels by BRAF kinase inhibitors were transient and they returned to the basal levels within 24 h, despite the phosphorylation of GCN2/eIF2α being kept at high levels (Figures 1A and S1A).

BRAF Depletion or Prolonged BRAF Kinase Inhibition Prevents ATF4 Induction

Unlike kinase inhibitors, siRNA-mediated knockdown of BRAF did not activate the GCN2-ATF4 pathway in A375 cells at any of the time points examined, although ERK phosphorylation declined in accordance with the decrease in BRAF expression (Figure 1C). Instead, BRAF knockdown prevented the induction of ATF4 expression but not GCN2 phosphorylation during additional challenge of 4-h treatments with BRAF kinase inhibitors (Figures 1D and S1B: alternative siRNA). Similarly, BRAF knockdown in A375 and G-361 cells prevented ATF4 induction but not GCN2/eIF2α phosphorylation under conditions of stress due to L-histidinol, a chemical stressor that mimics histidine deprivation through inhibiting histidyl tRNA synthetase (De Sousa-Coelho et al., 2013) (Figures 2A and S2A: alternative siRNA). In the case of glutamine deprivation, both GCN2/eIF2α phosphorylation and ATF4 induction were suppressed by BRAF knockdown (Figure 2B). Such preventive effects of BRAF knockdown on the GCN2-ATF4 pathway, especially ATF4 induction, were not seen in SK-MEL-2 and MeWo cells expressing wild-type BRAF (Figures 2A and 2B). Thus, depletion of oncogenic BRAF, but not wild-type BRAF, prevents ATF4 induction in response to BRAF kinase inhibitors as well as nutrient deprivation stress.

We also found that ATF4 induction during nutrient stress can be inhibited by prolonged pretreatments of A375 and G-361 cells with BRAF kinase inhibitors. Indeed, pretreatment with vemurafenib or dabrafenib for 24 h prevented ATF4 induction, without ERK reactivation, under stress conditions of L-histidinol addition and glutamine withdrawal, although GCN2/eIF2α phosphorylation remained high (Figures 2C, 2D, and
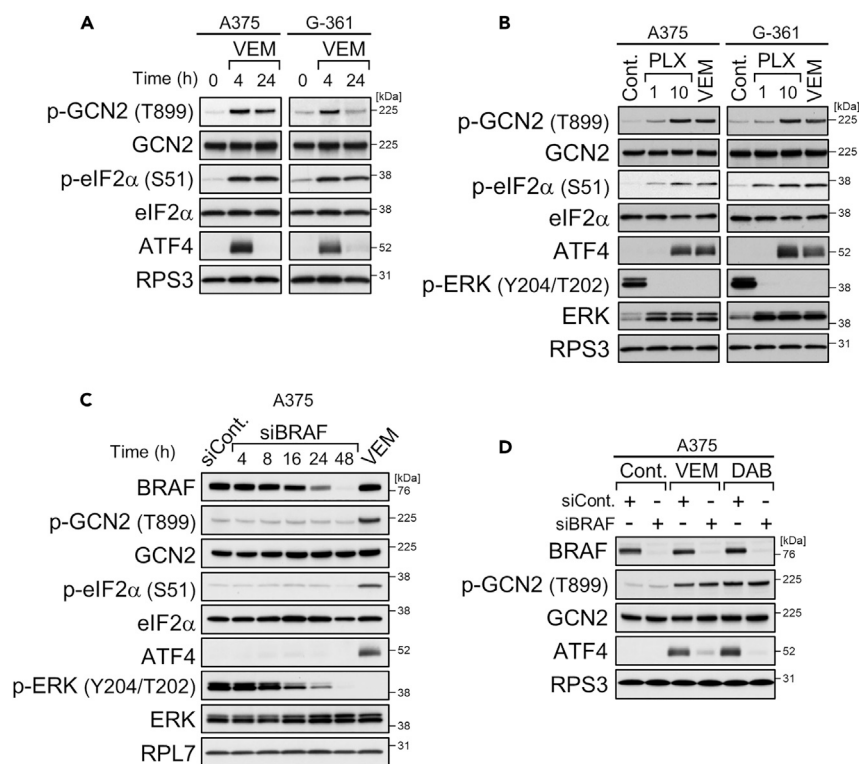
Figure 1. BRAF Kinase Inhibitors Induce ATF4 Expression Transiently

(A and B) Immunoblot analysis of A375 and G-361 cells treated with vemurafenib (VEM, 10 μM) for the indicated times (A) or vemurafenib (10 μM) or PLX7904 (PLX, 1, 10 μM) for 4 h (B).

(C and D) Immunoblot analysis of A375 cells with *BRAF* knockdown (C) and treatment with vemurafenib (10 μM) or dabrafenib (DAB, 1 μM) for 4 h (D).

See also Figure S1.

S2B). Thus, BRAF kinase inhibitors can exert biphasic effects on ATF4 expression: induction by short-term (4 h; see Figure 1) and inhibition by long-term (24 h) treatments, a unique property not seen for other stressors such as L-histidinol (Figure S2C).

Oncogenic BRAF Utilizes mTOR Signaling Pathway for ATF4 Induction

By treating A375 and G-361 cells with vemurafenib for 1 to 24 h, we found that the decay of ATF4 induction coincided with the attenuation of mTORC1 activity (Figure 3A). Unlike ERK dephosphorylation, the mTORC1 attenuation occurred relatively slowly. Actually, the phosphorylation levels of p70 ribosomal protein S6 kinase (p70 S6K) as well as its substrate ribosomal protein S6 (S6) (and, although less clearly, those of eIF4E binding protein 1 [4E-BP1]) steadily dropped from 8 h. Similar attenuation of mTORC1 activity was also provoked by BRAF knockdown in melanoma cells harboring oncogenic BRAF but not wild-type BRAF, as monitored by determining the phosphorylation status of S6 and 4E-BP1 (Figure 3B). Interestingly, compared with wild-type cells, BRAF-mutated cells showed resistance to L-histidinol-induced mTORC1 suppression, and this resistance was also diminished by BRAF knockdown (Figure 3B). Thus, the mTOR signaling pathway can be regulated by oncogenic BRAF under both normal and stress conditions.

To assess the involvement of mTOR in regulating ATF4 expression, we used different types of mTOR inhibitor. The selective and ATP-competitive mTOR inhibitor pp242 potently suppresses both mTORC1 and mTORC2, whereas the rapalogs rapamycin and everolimus moderately inhibit mTORC1 (Benjamin et al., 2011). Consistent with the mTOR-inhibitory potential, pp242 broadly prevented ATF4 induction under short-term treatments with vemurafenib or dabrafenib in BRAF-mutated cells (Figures 3D and S3C), as well as under conditions of stress due to L-histidinol in both wild-type and mutant cells (Figures 3C and S3A). Compared with those of pp242, the preventive effects of rapalogs were relatively weak and uneven depending on the stress types (Figures 3C–3E, S3B, and S3D). Conversely, mTORC1 activity and ATF4
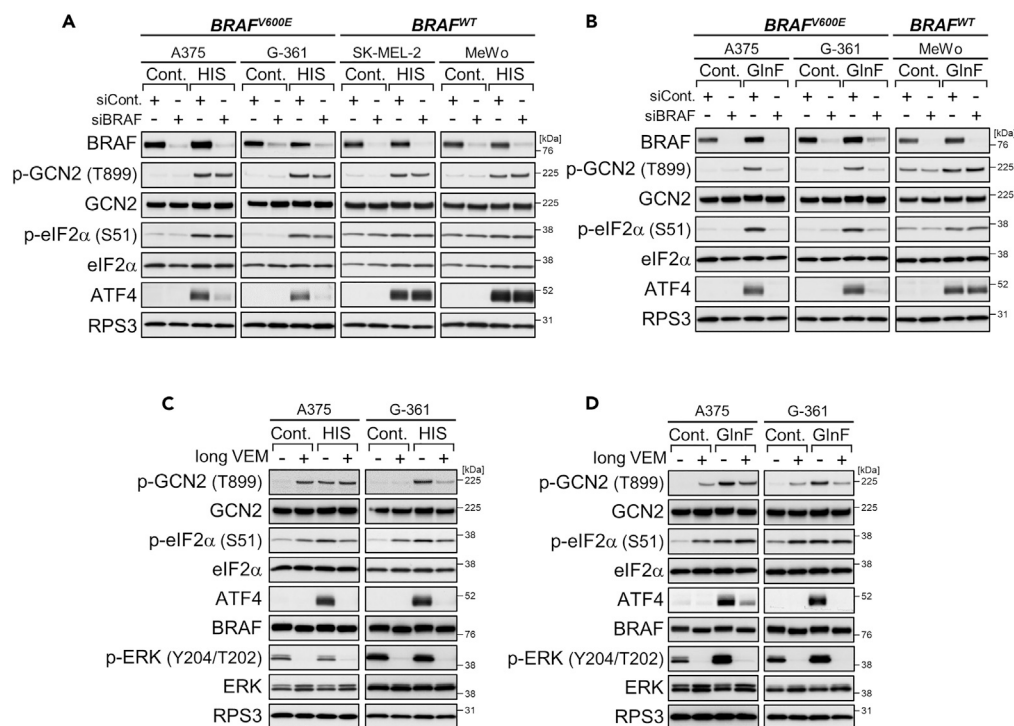
Figure 2. BRAF Depletion or Prolonged BRAF Kinase Inhibition Prevents ATF4 Induction

(A and B) Immunoblot analysis of the melanoma cell lines with *BRAF* knockdown and treatment with L-histidinol (HIS, 2 mM) for 4 h (A) or cultured in glutamine-free (GlnF) medium for 18 h (B).

(C) Immunoblot analysis of A375 and G-361 cells treated with vemurafenib (VEM, 10 μM) for 24 h and then treated with L-histidinol (2 mM) for 4 h.

(D) Immunoblot analysis of A375 and G-361 cells cultured in glutamine-free medium for 18 h in the presence or absence of vemurafenib (10 μM).

See also Figure S2.

expression were partially rescued by knockdown of Tuberous Sclerosis Complex 2 (TSC2), a negative regulator of mTORC1 (Inoki et al., 2002), under L-histidinol (but not vemurafenib [4 h]) stress in BRAF-silenced cells as well as under long-term vemurafenib treatment (16 h) in BRAF-unsilenced cells (Figures S3E and S3F). Although the precise reason remains unknown, the lack of rescue of ATF4 expression by TSC knockdown in BRAF-silenced, vemurafenib (4 h)-treated cells might be related to insufficient reactivation of mTORC1 owing to profound inhibition of the BRAF-mTOR axis. Notably, the ATF4 repression by mTOR inhibitors accompanied a tendency (especially in the case of pp242) to dampen GCN2/eIF2α phosphorylation, suggesting cross talk between the mTOR and GCN2 pathways. Taken together, these results indicate that oncogenic BRAF utilizes mTOR as a downstream regulator of ATF4 expression.

Oncogenic BRAF Enhances eIF4B Phosphorylation for ATF4 Induction

During the above time course experiments with vemurafenib (see Figure 3A), delayed attenuation similar to that in the mTOR signaling pathway was observed in phosphorylation (Ser422) for the activation of eIF4B (Figure 4A), an accessory factor stimulating eIF4A RNA helicase (Rozovsky et al., 2008). BRAF knockdown also lowered the phosphorylation levels of eIF4B in BRAF-mutated cells specifically (Figures 4B and S4A: alternative siRNA). Conversely, overexpression of mutant BRAF, but not the wild-type, enhanced eIF4B phosphorylation levels (Figure 4C). However, eIF4B phosphorylation in A375 cells was not affected by mTOR inhibition or the inhibition of other BRAF downstream kinases MEK and Akt with each of the selective inhibitors (Figure S4B). Thus, eIF4B phosphorylation can be under the control of oncogenic BRAF but not wild-type BRAF, possibly in a manner independent of MEK, Akt, and mTOR.

Interestingly, eIF4B knockdown in A375 and G-361 cells attenuated ATF4 induction under conditions of short-term treatments with BRAF kinase inhibitors (Figures 4D and S4C: alternative siRNA) but not under
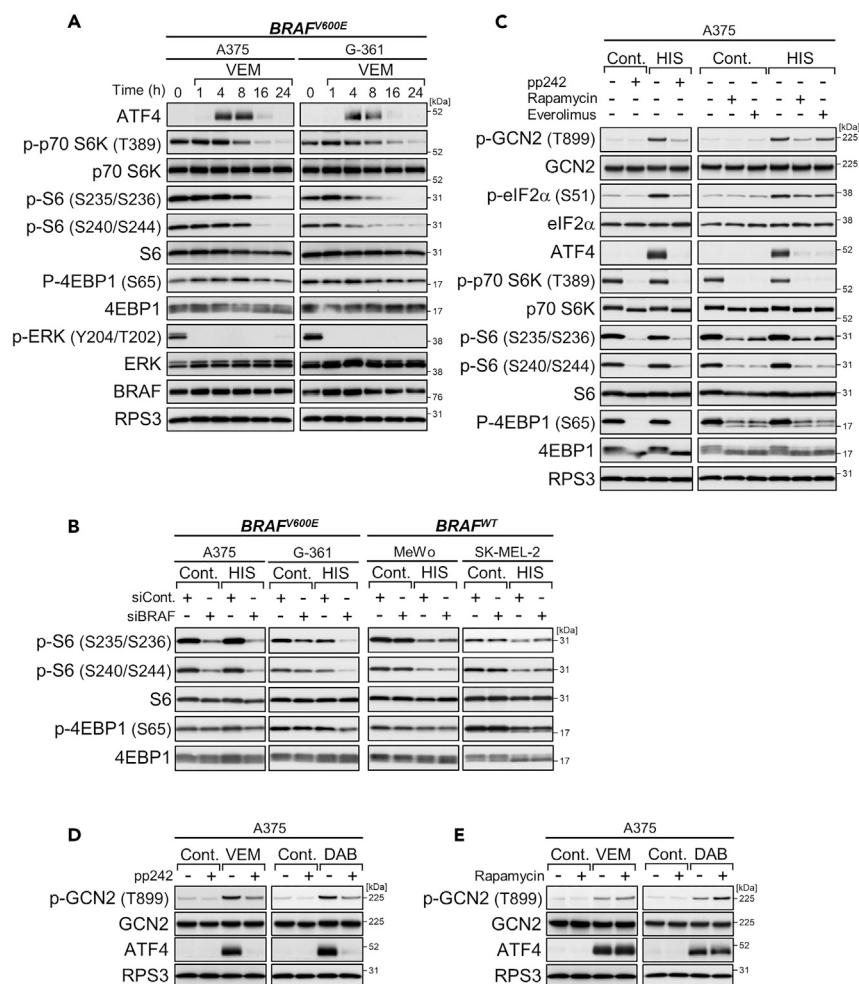
Figure 3. Oncogenic BRAF Utilizes mTOR Signaling Pathway for ATF4 Induction

(A) Immunoblot analysis of A375 and G-361 cells treated with vemurafenib (VEM, 10 μM) for the indicated times.

(B) Immunoblot analysis of the melanoma cell lines with *BRAF* knockdown and treatment with L-histidinol (HIS, 2 mM) for 4 h. The internal control bands are shown in Figure 2A.

(C) Immunoblot analysis of A375 cells treated with L-histidinol (2 mM) alone or in combination with pp242 (1 μM), rapamycin (0.1 μM), or everolimus (0.1 μM) for 4 h.

(D and E) Immunoblot analysis of A375 cells treated with vemurafenib (10 μM) or dabrafenib (DAB, 1 μM) alone or in combination with pp242 (1 μM) (D) or rapamycin (0.1 μM) (E) for 4 h.

See also Figure S3.

nutrient stress conditions of L-histidinol addition and glutamine withdrawal (Figures 4E and S4D). This selectivity in ATF4 attenuation was more consistent with the decrease in phosphorylation levels of eIF4B rather than the levels of eIF4B or the GCN2/eIF2α phosphorylation state, raising the possibility that the loss of residual eIF4A-stimulating activity by dephosphorylation may be needed to attenuate ATF4 induction. Actually, hampering eIF4A with specific siRNAs or the selective inhibitor silvestrol impaired ATF4 induction very broadly, in both wild-type and mutant BRAF cells, under all conditions examined, including not only GCN2-activating (BRAF inhibitors and L-histidinol) but also PERK-activating conditions (tunicamycin and thapsigargin) (Figures 4F, 4G, and S4E–S4H). Thus, eIF4A likely functions as basic machinery for ATF4 translation under stress conditions. Taking these findings together, eIF4B, especially active, phosphorylated forms, appears to be involved in ATF4 induction, possibly through regulating the eIF4A-dependent translation in BRAF-mutated melanoma cells. Notably, this eIF4B-ATF4 axis may also contribute to cell survival upon BRAF inhibition because eIF4B knockdown can slightly but significantly enhance cellular sensitivity to vemurafenib (Figure S4I), as previously shown with ATF4 knockdown (Nagasawa et al., 2017).
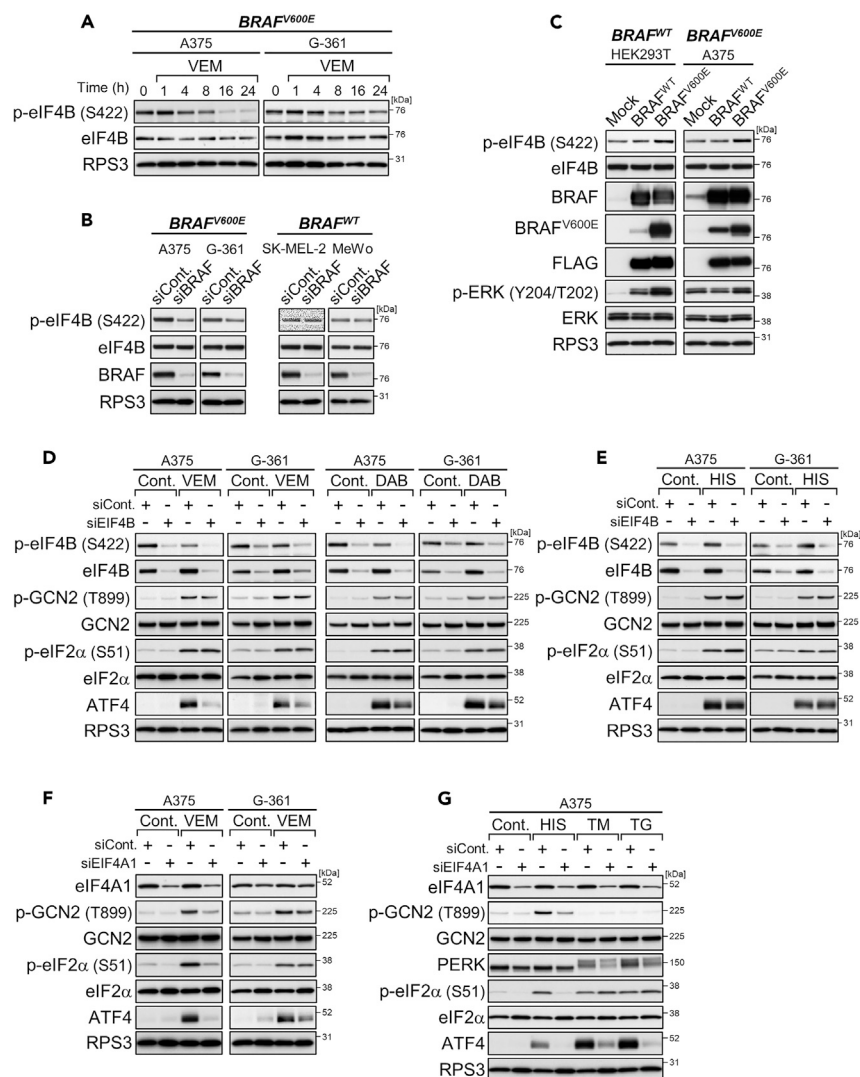
Figure 4. Oncogenic BRAF Enhances eIF4B Phosphorylation for ATF4 Induction

(A) Immunoblot analysis of A375 and G-361 cells treated with vemurafenib (VEM, 10 μM) for the indicated times.

(B) Immunoblot analysis of the melanoma cell lines with *BRAF* knockdown.

(C) Immunoblot analysis of HEK293T and A375 cells with overexpression of wild-type BRAF or mutant BRAF.

(D and E) Immunoblot analysis of A375 and G-361 cells with *EIF4B* knockdown and treatment with vemurafenib (10 μM) or dabrafenib (DAB, 1 μM) (D) or with L-histidinol (HIS, 2 mM) (E) for 4 h.

(F and G) Immunoblot analysis of A375 and G-361 cells with *EIF4A1* knockdown and treated with vemurafenib (10 μM) (F) or with L-histidinol (2 mM), tunicamycin (TM, 1 μg/mL), or thapsigargin (TG, 0.3 μM) (G) for 4 h.

See also Figure S4.

Expression of ATF4 Target Genes Is Influenced by BRAF Inhibition

Gene expression analysis of A375 cells treated with vemurafenib for 6 or 16 h, or silenced with siRNA specific for BRAF, revealed that 3,214 probe sets, representing genes that are involved in various cellular processes, were altered more than 2-fold by either perturbation (Figure 5A and Tables S1 and S2). These gene expression changes were very similar and, indeed, the directions of expression changes were highly concordant between the BRAF-inhibiting perturbations (61.8%–82.4% concordance rates; Figure S5A). Notably, somewhat distinct changes in expression of particular gene sets were seen between vemurafenib treatment and BRAF knockdown (e.g., clusters 2–4 in Figure 5A), possibly, at least in some cases, reflecting the different modes of action of each perturbation (kinase inhibition versus protein depletion). As part of the effectiveness evaluation, BRAF knockdown was also found to suppress the transcriptional response in
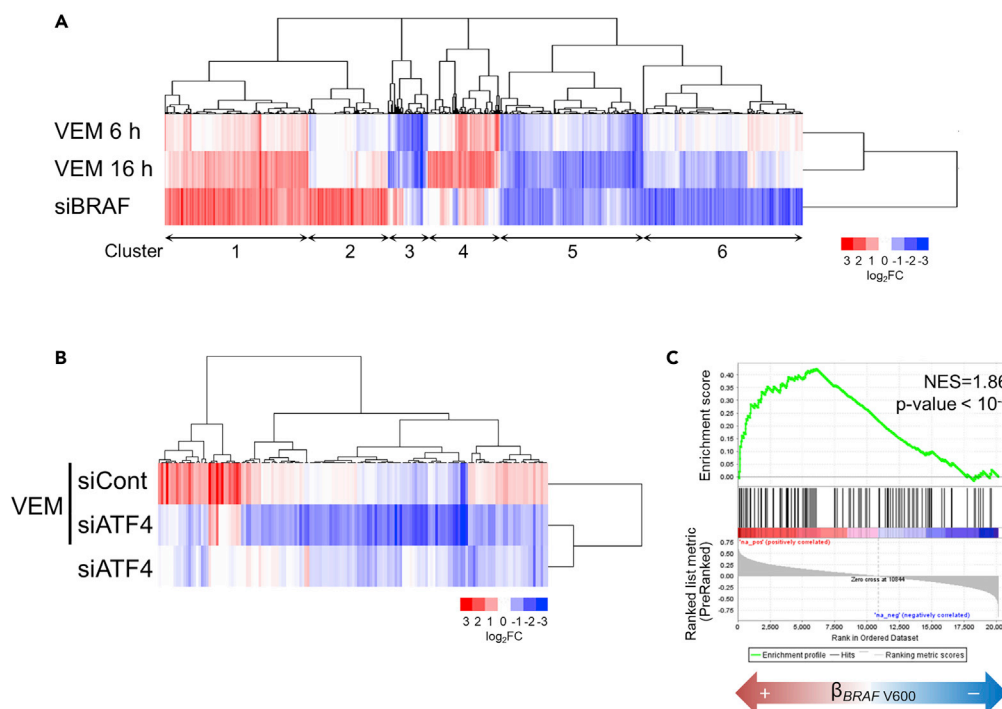
Figure 5. Expression of ATF4 Target Genes Is Influenced by BRAF Inhibition

(A) Signature of 3,214 probe sets (2,311 genes) that were either upregulated or downregulated by treatment with vemurafenib (VEM, 10 μM, 6 or 16 h) or *BRAF* knockdown in A375 cells. The log2 fold change of levels under the indicated conditions is shown for the condition of treatment with DMSO (for vemurafenib treatment) or transfection with nontargeting siRNA (siCont) (for *BRAF* knockdown). For probe lists and GO analysis results, see Tables S1 and S2.

(B) Signature of 155 probe sets (116 genes) that were downregulated by *ATF4* knockdown during treatment with vemurafenib (10 μM) for 4 h in A375 cells. The log2 fold change of levels under the indicated conditions is shown for the condition of transfection with nontargeting siRNA and then treatment with DMSO. For probe lists, see Table S5.

(C) Enrichment plot of GSEA using the 107 genes defined from the BRAFi-ATF4 signature. We tested the enrichment of these genes in transcripts upregulated by BRAF V600 mutation in human melanomas. NES, normalized enrichment score. For gene lists, see Table S7. See also Figure S5.

A375 cells deprived of glutamine (Figure S5B and Table S3), in line with the above findings that oncogenic BRAF regulates the ISR signaling pathway during nutrient stress.

Comparison of changes in gene expression upon vemurafenib treatment (4 h) with or without ATF4 knockdown suggested that ATF4 exerted only limited effects on the transcriptional response to vemurafenib in A375 cells (Figures S5C and S5D, and Table S4). We then extracted 155 probe sets (116 genes) as a BRAFi-ATF4 signature that was downregulated by ATF4 knockdown under vemurafenib treatment (Figure 5B and Table S5). Consistent with the time course changes in ATF4 levels (see Figure 3A), the BRAFi-ATF4 signature, especially 72 probe sets (56 genes) that overlapped with those altered by BRAF-inhibiting perturbations as above (Figure 5A), had a tendency to show lower expression levels at 16 h than at 6 h during vemurafenib treatment (Figure S5E and Table S6). Remarkably, the majority of 72 probe sets (56 genes) were downregulated by BRAF knockdown (Figure S5E). Furthermore, gene set enrichment analysis, using a public melanoma gene expression dataset, revealed that the BRAFi-ATF4 signature was highly enriched in melanoma harboring BRAF V600 mutations ($p < 10^{-4}$) (Figure 5C and Table S7). Thus, oncogenic BRAF-mediated regulation of ATF4 target genes can be clinically relevant in melanoma.

Identification of a Chemical Compound that Suppresses GCN2-ATF4 Pathway Activation during BRAF Kinase Inhibition

By screening of a kinase inhibitor library with fluorescent immunostaining of ATF4, we identified a multi-kinase inhibitor, AT9283 (Figure 6A), that selectively prevented nuclear ATF4 accumulation induced by BRAF kinase inhibitors (Figure 6B). AT9283 dose-dependently inhibited GCN2/eIF2α phosphorylation induced
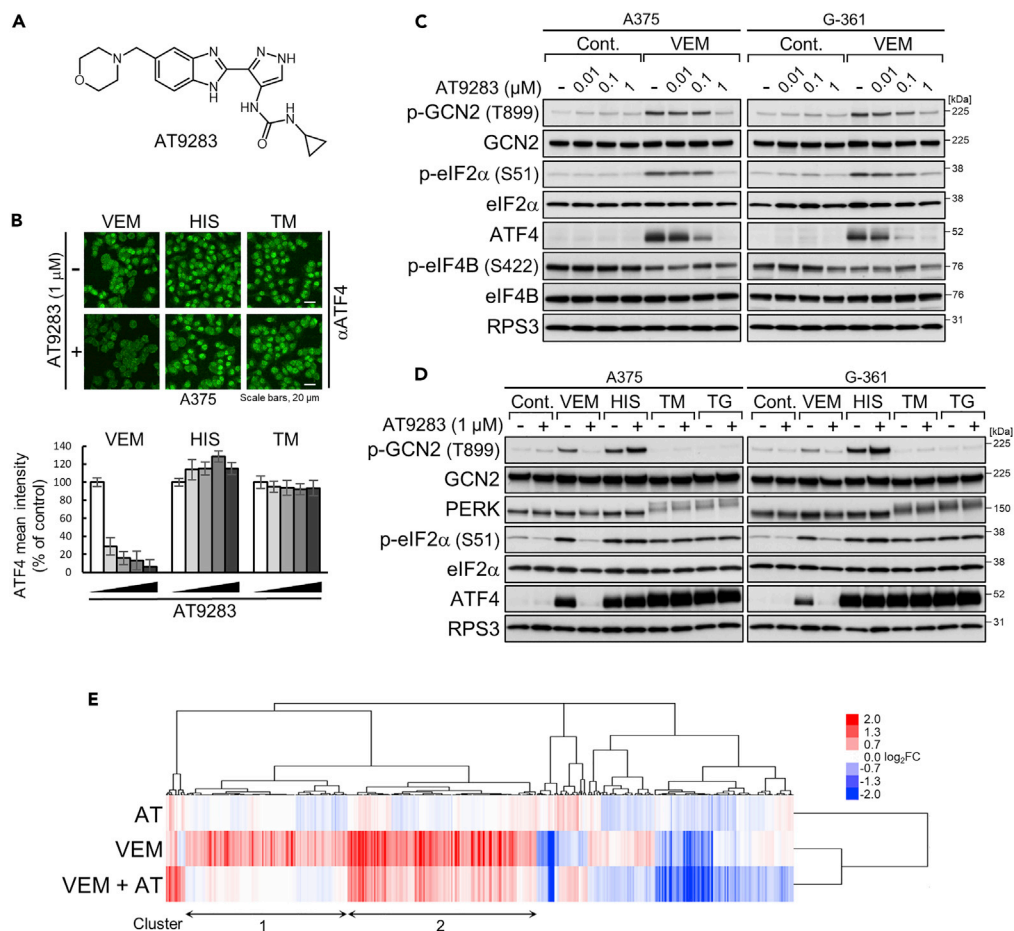
Figure 6. Identification of a Chemical Compound that Suppresses GCN2-ATF4 Pathway Activation during BRAF Kinase Inhibition

(A) Chemical structure of AT9283.

(B) A375 cells were treated with vemurafenib (VEM, 10 μM), L-histidinol (HIS, 2 mM), or tunicamycin (TM, 1 μg/mL) in the presence or absence of AT9283 (0.1, 0.2, 0.5, or 1 μM) for 6 h. The cells were fixed and stained with anti-ATF4 antibody (green). Bars represent the quantification of the intensity of ATF4 signals in the nucleus. Results are shown as the mean ± SD (n = 6).

(C and D) Immunoblot analysis of A375 and G-361 cells treated with AT9283 alone or in combination with vemurafenib (10 μM), L-histidinol (2 mM), tunicamycin (1 μg/mL), or thapsigargin (TG, 0.3 μM) for 4 h.

(E) Signature of 432 probe sets (309 genes) whose expression levels were upregulated or downregulated by combined treatment with vemurafenib (10 μM) and AT9283 (0.1 μM) for 6 h compared with the level upon treatment with vemurafenib alone for 6 h in A375 cells. The log2 fold change of levels under the indicated conditions is shown for the condition of treatment with DMSO. For probe lists and GO analysis results, see Tables S8 and S9.

See also Figure S6.

by vemurafenib (Figure 6C) in A375 and G-361 cells and by dabrafenib (Figure S6A) in A375 cells, but did not inhibit GCN2/eIF2α phosphorylation induced by nutrient stresses (Figures 6D and S6B) and also PERK/eIF2α phosphorylation induced by tunicamycin or thapsigargin (Figure 6D). The prevention of ATF4 induction occurred with only marginal effects on the phosphorylation levels of eIF4B and S6 (Figures 6C and S6C) and was not recaptured by other kinase inhibitors targeting known AT9283-inhibitable kinases, such as Abl, JAK2/3, and Aurora (Howard et al., 2009) (Figure S6D). Gene expression analysis of A375 cells further supported GCN2-ATF4 pathway inhibition. Indeed, AT9283 counteracted vemurafenib (6 h)-induced activation of ATF4-target genes (p < 10^{-4} by Enrichr online tool with the Reactome pathway database for cluster 1 and 2 in Figure 6E) (Chen et al., 2013; Gjymishka et al., 2009; Kuleshov et al., 2016), especially ASNS, PSAT1, and PSPH that are well-known ATF4 targets involved in amino acid metabolism (Tables S8 and S9) (Adams, 2007). Consistently, AT9283 led to the downregulation of gene
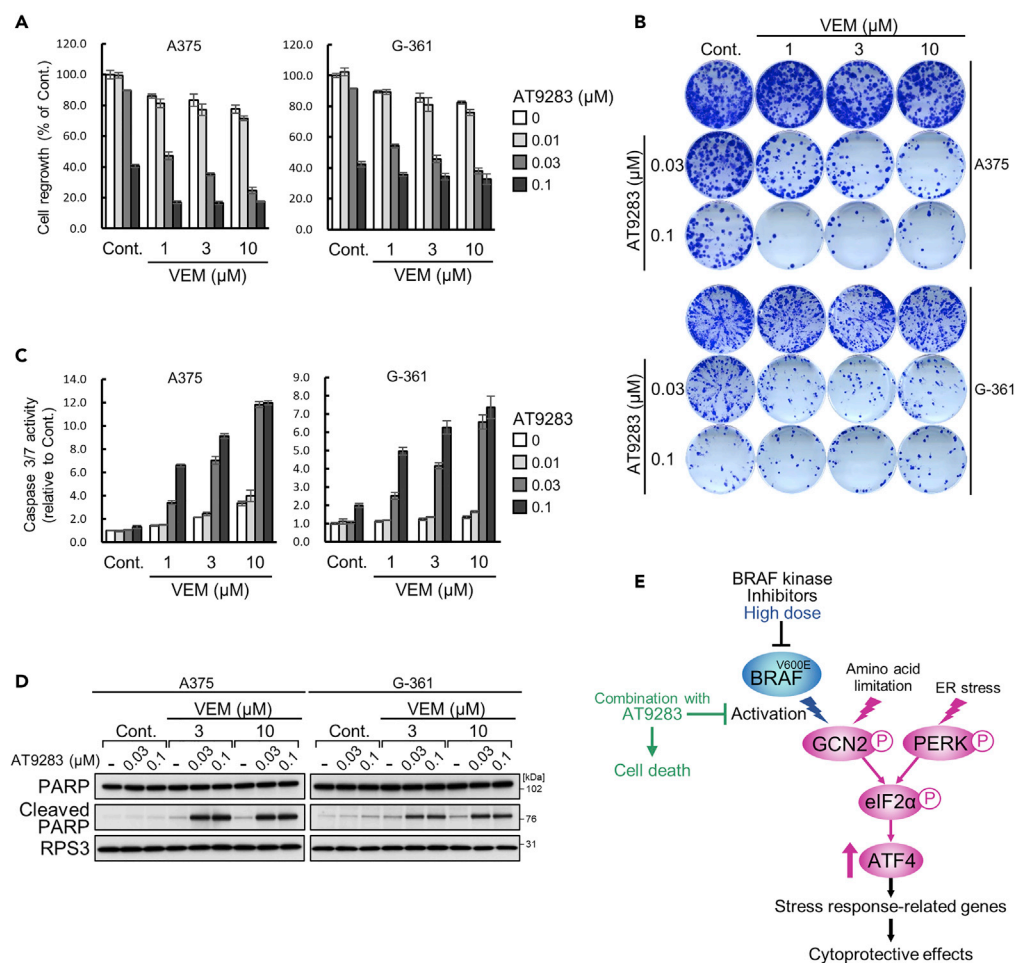
Figure 7. Enhanced Growth Inhibition by Combined Treatments with BRAF Inhibitors and AT9283

(A and B) A375 and G-361 cells were treated with AT9283 alone or in combination with vemurafenib (VEM) for 16 h. The cells were reseeded in 96-well plates (A) or 6-well plates (B) and cultured in drug-free medium for 96 h (A), or 7 (A375) or 14 (G-361) days (B). Results are shown as the mean ± SD (n = 3).

(C) A375 and G-361 cells were treated with AT9283 alone or in combination with vemurafenib for 16 h. The caspase-3/7 activities were measured by the Caspase-Glo 3/7 assay. Results are shown as the mean ± SD (n = 3).

(D) Immunoblot analysis of A375 and G-361 cells treated with AT9283 alone or in combination with vemurafenib for 16 h.

(E) Mechanisms of AT9283 involved in prevention of the GCN2-ATF4 pathway activation by BRAF kinase inhibitors.

See also Figure S7.

expression broadly in the BRAFi-ATF4 signature (86% and 62% of probe sets up- and downregulated by vemurafenib, respectively) (Figure S6E). Thus, AT9283 effectively prevents activation of the GCN2-ATF4 pathway in response to BRAF inhibitors.

Combined treatment with vemurafenib and AT9283 for 16 h led to profound growth inhibition in A375 and G-361 cells when the cell growth ability was assessed by reseeding and culturing cells in fresh medium for 96 h or until colony formation (Figures 7A and 7B). During the drug treatments, cell attachment was largely unaffected, although a decrease in cell number was seen (Figure S7C). In fact, in the BRAF-mutated cell lines, AT9283 also enhanced apoptosis induction in combination with vemurafenib or dabrafenib for 16 h, as determined by increased caspase 3/7 activity and PARP cleavage (Figures 7C, 7D, S7A, and S7B). The effects of AT9283, however, were not phenocopied by other kinase inhibitors targeting Abl, JAK2/3, Aurora, or their combinations (Figure S7D). In addition, such enhancement of apoptosis induction by AT9283 was not seen in BRAF wild-type cells co-treated with vemurafenib (Figure S7E) or in BRAF mutant cells co-treated with L-histidinol (Figure S7F). These results indicate that AT9283 can induce vulnerability to BRAF kinase inhibitors in BRAF-mutated melanoma cells (Figure 7E).

DISCUSSION

Using melanoma cell lines with BRAF^{V600E} mutation, we have shown that oncogenic BRAF signaling controls the expression of ATF4, the major ISR transcription factor. Indeed, siRNA-mediated knockdown of BRAF prevents ATF4 induction during nutrient stress. ATF4 induction is also inhibited by relatively long-term treatments (16–24 h) with the BRAF kinase inhibitors vemurafenib and dabrafenib. Thus, oncogenic BRAF positively regulates ATF4 expression. We further identified mTOR and eIF4B as downstream regulators in BRAF-mediated ATF4 regulation. Curiously, ATF4 was rapidly induced by short-term treatments (4–8 h) with BRAF kinase inhibitors, depending on the stress kinase GCN2 (Nagasawa et al., 2017), before onset of the downregulation of mTOR and eIF4B. This paradoxical response was effectively inhibited by a small compound, resulting in sensitization to BRAF kinase inhibitors. Taken together, our findings indicate that oncogenic BRAF-mediated regulation of ATF4 expression plays a central role in stress response and cell survival.

In addition to BRAF, several oncogenes or oncogenic signals have been shown to regulate ATF4 expression (Gwinn et al., 2018; Heydt et al., 2018; Zhao et al., 2016). Although ATF4 can be cytoprotective and proapoptotic depending on the cell conditions (Pakos-Zebrucka et al., 2016), loss of ATF4 has been repeatedly shown to suppress tumor growth in xenograft models (Dey et al., 2015; Ye et al., 2010). In line with this, increased expression of ATF4 has been observed in certain tumors in clinical settings (Chen et al., 2017; Dey et al., 2015). Using a TCGA dataset, we also found that the BRAFi-ATF4 signature, an ATF4-regulated gene set defined under short-term BRAF kinase inhibition, is enriched in BRAF-mutated tumors derived from patients with skin cutaneous melanoma (Figure 5C). Thus, it is conceivable that the BRAF-ATF4 axis contributes to tumor formation in malignant melanoma, possibly through modulating the transcriptional response to nutrient status in tumors. Indeed, oncogenic BRAF modulates various types of cellular metabolism (Haq et al., 2013; Kang et al., 2015), and we demonstrated that knockdown of BRAF not only prevents ATF4 induction but also abrogates transcriptional alterations in response to glutamine deprivation (Figure S5B). Similar oncogenic regulation of glutamine response has been seen in KRAS mutant lung cancer, and in those cells, KRAS regulates ATF4 expression to support amino acid homeostasis (Gwinn et al., 2018). These observations collectively suggest that oncogene-mediated regulation of ATF4 can be a common mechanism to manage metabolic homeostasis, particularly amino acid metabolism, in tumors.

It is conceivable that mTOR and eIF4B, as downstream regulators of oncogenic BRAF, cooperate to regulate ATF4 expression. Actually, both proteins, in common, modulate the eIF4F translation initiation complex, consisting of the eIF4E cap-binding protein, the eIF4G scaffolding protein, and the eIF4A RNA helicase (Silvera et al., 2010). Inhibition of mTOR kinase can lead to disruption of the eIF4F complex by activating 4E-BP1 that blocks eIF4E-eIF4G interaction (Richter and Sonenberg, 2005), whereas inactivation of eIF4B can lead to loss of function to stimulate eIF4A activity (Rozovsky et al., 2008). In agreement with this, 4E-BP1 can negatively regulate ATF4 expression under the control of mTORC1 (Park et al., 2017), and, as we showed herein, inactivation of eIF4A can prevent ATF4 induction. Thus, the eIF4F complex is likely one of the focal points where oncogenic BRAF effectively regulates ATF4 expression. In this regard, persistent formation of active eIF4F complex has been identified as a mechanism for both innate and acquired resistance to BRAF-targeted therapy (Boussemart et al., 2014). Together with this, our present findings raise the possibility that control of ATF4 translation initiation through the eIF4F complex plays an important role in resistance to BRAF-targeted therapy.

Contrary to relatively long-term treatments (16–24 h), short-term treatments (4–8 h) with BRAF kinase inhibitors paradoxically lead to GCN2 activation and subsequent induction of ATF4. Importantly, ATF4 knockdown enhances cellular sensitivity to the anti-proliferative effect of vemurafenib (Nagasawa et al., 2017), suggesting that the GCN2-mediated ATF4 induction functions as part of the cellular stress response to BRAF inhibition. Consistent with this notion, we herein found that the BRAFi-ATF4 signature contained many genes expressed in a BRAF-dependent manner (Figure S5E). In this context, it would be conceivable that abrupt inhibition of BRAF kinase activity, *per se*, becomes a stressor to trigger the GCN2-ATF4 stress response pathway. Actually, in the presence of BRAF kinase inhibitors, paradoxical induction of ATF4 occurs after the rapid inhibition of ERK phosphorylation and continues until the onset of mTOR and eIF4B inhibition, which can lead to prevention of the translation initiation of ATF4 as above. Thus, differential regulation of the ERK and mTOR/eIF4B signaling pathways during BRAF kinase inhibition may provide a time window that enables cells to activate the GCN2-mediated stress response and induce ATF4 transiently. However, it is likely that activation of the GCN2-ATF4 pathway is uncoupled from the MEK-ERK pathway inhibition, as the MEK inhibitor trametinib does not activate the GCN2-ATF4 pathway in BRAF-mutated cells (Nagasawa et al., 2017).

Finally, we found that rapid activation of the GCN2-ATF4 pathway by BRAF kinase inhibitors can be effectively prevented by AT9283, a broad-spectrum kinase inhibitor that inhibits kinases such as JAK2, JAK3, Aurora A, Aurora B, and c-ABL (Howard et al., 2009). Our efforts to drive clinical applications of this finding, including to identify the target kinase(s) of AT9283 for this unexpected property and to determine the appropriate conditions for its administration to tumor-bearing mice, have been unsuccessful. Nonetheless, our results already show that AT9283 possesses unique features as a lead compound against BRAF-mutated cells. The prevention of GCN2-ATF4 pathway activation by this compound has been seen selectively in BRAF-mutated cells treated with BRAF kinase inhibitors, but not with amino acid stress, revealing that different signaling mechanisms can operate between each type of stressor. In agreement with this, combinations of AT9283 with BRAF kinase inhibitors, but not with amino acid stress, lead to the synergistic induction of apoptosis in BRAF-mutated cells. Meanwhile, the potent efficacy of AT9383, as compared with that of ATF4 knockdown (Nagasawa et al., 2017), suggests that the synergistic apoptosis induction may be attributed to ATF4-dependent and -independent mechanisms.

In fact, although somewhat less effective, AT9283 can also enhance apoptosis induction in combination with the MEK inhibitor trametinib (Figure S7G). This observation, together with the fact that trametinib does not activate the GCN2-ATF4 pathway (Nagasawa et al., 2017), suggests that mechanisms other than preventing ATF4 induction are also involved in the enhanced cell death by combined treatments with BRAF inhibitors and AT9283. Although further studies are needed to understand the whole mechanisms of AT9283-induced apoptosis during BRAF inhibition, these features shed light on the existence of druggable mechanisms to improve melanoma therapy using BRAF inhibitor together with or without MEK inhibitor. A deeper understanding of the mechanisms for GCN2-ATF4 pathway activation upon the acute inhibition of BRAF kinase activity, as well as for oncogenic BRAF-mediated ATF4 regulation, would provide a novel therapeutic strategy to combat melanoma harboring mutated BRAF.

Limitations of the Study

We demonstrated that oncogenic BRAF promotes cellular stress adaptation by collaborating with the ISR pathway and that disruption of this collaborative, adaptive mechanism results in sensitization of melanoma cells to BRAF inhibitors. However, the detailed mechanisms of BRAF-driven stress adaptation as well as BRAF inhibitor-induced ISR activation remain to be fully elucidated. The chemical compound, which we identified to inhibit activation of the ISR and to sensitize melanoma cells to BRAF inhibitors, may have pleiotropic, as-yet-unidentified mechanisms of action. Although we showed that the expression of ISR target genes is enriched in BRAF-mutated melanomas, future studies will be needed to determine the clinical relevance of our findings and their potential implications in BRAF-targeted therapy.

METHODS

All methods can be found in the accompanying Transparent Methods supplemental file.

DATA AND CODE AVAILABILITY

The accession number for the microarray data reported in this paper is National Center for Biotechnology Information Gene Expression Omnibus: GSE136615.

SUPPLEMENTAL INFORMATION

Supplemental Information can be found online at https://doi.org/10.1016/j.isci.2020.101028.

ACKNOWLEDGMENTS

AUTHOR CONTRIBUTIONS

I.N. and A.T. conceived the study and analyzed the data. I.N. and Y.T. performed immunoblot analysis. S.T. and K.K. performed microarray experiments. M.K. performed gene expression profiling. I.N. performed other experiments. I.N. and A.T. wrote the manuscript.

DECLARATION OF INTERESTS

REFERENCES

Adams, C.M. (2007). Role of the transcription factor ATF4 in the anabolic actions of insulin and the anti-anabolic actions of glucocorticoids. J. Biol. Chem. 282, 16744–16753.

Baenke, F., Chaneton, B., Smith, M., Van Den Broek, N., Hogan, K., Tang, H., Viros, A., Martin, M., Galbraith, L., Girotti, M.R., et al. (2016). Resistance to BRAF inhibitors induces glutamine dependency in melanoma cells. Mol. Oncol. 10, 73–84.

Benjamin, D., Colombi, M., Moroni, C., and Hall, M.N. (2011). Rapamycin passes the torch: a new generation of mTOR inhibitors. Nat. Rev. Drug Discov. 10, 868–880.

Boussemart, L., Malka-Mahieu, H., Girault, I., Allard, D., Hemmingsson, O., Tomasic, G., Thomas, M., Basmadjian, C., Ribeiro, N., Thuaud, F., et al. (2014). eIF4F is a nexus of resistance to anti-BRAF and anti-MEK cancer therapies. Nature 513, 105–109.

Bradley, S.D., Melendez, B., Talukder, A., and Lizee, G. (2016). Trouble at the core: BRAF(V600E) drives multiple modes of T-cell suppression in melanoma. Oncoimmunology 5, e1078966.

Chapman, P.B., Hauschild, A., Robert, C., Haanen, J.B., Ascierto, P., Larkin, J., Dummer, R., Garbe, C., Testori, A., Maio, M., et al. (2011). Improved survival with vemurafenib in melanoma with BRAF V600E mutation. N. Engl. J. Med. 364, 2507–2516.

Chen, D., Fan, Z., Rauh, M., Buchfelder, M., Eyupoglu, I.Y., and Savaskan, N. (2017). ATF4 promotes angiogenesis and neuronal cell death and confers ferroptosis in a xCT-dependent manner. Oncogene 36, 5593–5608.

Chen, E.Y., Tan, C.M., Kou, Y., Duan, Q., Wang, Z., Meirelles, G.V., Clark, N.R., and Ma'ayan, A. (2013). Enrichr: interactive and collaborative HTML5 gene list enrichment analysis tool. BMC Bioinformatics 14, 128.

Das Thakur, M., and Stuart, D.D. (2014). Molecular pathways: response and resistance to BRAF and MEK inhibitors in BRAF(V600E) tumors. Clin. Cancer Res. 20, 1074–1080.

Davies, H., Bignell, G.R., Cox, C., Stephens, P., Edkins, S., Clegg, S., Teague, J., Woffendin, H., Garnett, M.J., Bottomley, W., et al. (2002).

Mutations of the BRAF gene in human cancer. Nature 417, 949–954.

De Sousa-Coelho, A.L., Relat, J., Hondares, E., Perez-Marti, A., Ribas, F., Villarroya, F., Marrero, P.F., and Haro, D. (2013). FGF21 mediates the lipid metabolism response to amino acid starvation. J. Lipid Res. 54, 1786–1797.

Dey, S., Sayers, C.M., Verginadis, , II, Lehman, S.L., Cheng, Y., Cerniglia, G.J., Tuttle, S.W., Feldman, M.D., Zhang, P.J., Fuchs, S.Y., et al. (2015). ATF4-dependent induction of heme oxygenase 1 prevents anoikis and promotes metastasis. J. Clin. Invest. 125, 2592–2608.

Falchook, G.S., Long, G.V., Kurzrock, R., Kim, K.B., Arkenau, H.T., Brown, M.P., Hamid, O., Infante, J.R., Millward, M., Pavlick, A., et al. (2014). Dose selection, pharmacokinetics, and pharmacodynamics of BRAF inhibitor dabrafenib (GSK2118436). Clin. Cancer Res. 20, 4449–4458.

Flaherty, K.T., Puzanov, I., Kim, K.B., Ribas, A., McArthur, G.A., Sosman, J.A., O'Dwyer, P.J., Lee, R.J., Grippo, J.F., Nolop, K., et al. (2010). Inhibition of mutated, activated BRAF in metastatic melanoma. N. Engl. J. Med. 363, 809–819.

Gjymishka, A., Su, N., and Kilberg, M.S. (2009). Transcriptional induction of the human asparagine synthetase gene during the unfolded protein response does not require the ATF6 and IRE1/XBP1 arms of the pathway. Biochem. J. 417, 695–703.

Gwinn, D.M., Lee, A.G., Briones-Martin-Del-Campo, M., Conn, C.S., Simpson, D.R., Scott, A.I., Le, A., Cowan, T.M., Ruggero, D., and Sweet-Cordero, E.A. (2018). Oncogenic KRAS regulates amino acid homeostasis and asparagine biosynthesis via ATF4 and alters sensitivity to L-asparaginase. Cancer Cell 33, 91–107.e106.

Hangauer, M.J., Viswanathan, V.S., Ryan, M.J., Bole, D., Eaton, J.K., Matov, A., Galeas, J., Dhruv, H.D., Berens, M.E., Schreiber, S.L., et al. (2017). Drug-tolerant persister cancer cells are vulnerable to GPX4 inhibition. Nature 551, 247–250.

Haq, R., Shoag, J., Andreu-Perez, P., Yokoyama, S., Edelman, H., Rowe, G.C., Frederick, D.T., Hurley, A.D., Nellore, A., Kung, A.L., et al. (2013). Oncogenic BRAF regulates oxidative metabolism

via PGC1alpha and MITF. Cancer Cell 23, 302–315.

Hatzivassiliou, G., Song, K., Yen, I., Brandhuber, B.J., Anderson, D.J., Alvarado, R., Ludlam, M.J., Stokoe, D., Gloor, S.L., Vigers, G., et al. (2010). RAF inhibitors prime wild-type RAF to activate the MAPK pathway and enhance growth. Nature 464, 431–435.

Hernandez-Davies, J.E., Tran, T.Q., Reid, M.A., Rosales, K.R., Lowman, X.H., Pan, M., Moriceau, G., Yang, Y., Wu, J., Lo, R.S., et al. (2015). Vemurafenib resistance reprograms melanoma cells towards glutamine dependence. J. Transl. Med. 13, 210.

Heydt, Q., Larrue, C., Saland, E., Bertoli, S., Sarry, J.E., Besson, A., Manenti, S., Joffre, C., and Mansat-De Mas, V. (2018). Oncogenic FLT3-ITD supports autophagy via ATF4 in acute myeloid leukemia. Oncogene 37, 787–797.

Howard, S., Berdini, V., Boulstridge, J.A., Carr, M.G., Cross, D.M., Curry, J., Devine, L.A., Early, T.R., Fazal, L., Gill, A.L., et al. (2009). Fragment-based discovery of the pyrazol-4-yl urea (AT9283), a multitargeted kinase inhibitor with potent aurora kinase activity. J. Med. Chem. 52, 379–388.

Inoki, K., Li, Y., Zhu, T., Wu, J., and Guan, K.L. (2002). TSC2 is phosphorylated and inhibited by Akt and suppresses mTOR signalling. Nat. Cell Biol. 4, 648–657.

Kang, H.B., Fan, J., Lin, R., Elf, S., Ji, Q., Zhao, L., Jin, L., Seo, J.H., Shan, C., Arbiser, J.L., et al. (2015). Metabolic rewiring by oncogenic BRAF V600E links ketogenesis pathway to BRAF-MEK1 signaling. Mol. Cell 59, 345–358.

Kuleshov, M.V., Jones, M.R., Rouillard, A.D., Fernandez, N.F., Duan, Q., Wang, Z., Koplev, S., Jenkins, S.L., Jagodnik, K.M., Lachmann, A., et al. (2016). Enrichr: a comprehensive gene set enrichment analysis web server 2016 update. Nucleic Acids Res. 44, W90–W97.

Nagasawa, I., Kunimasa, K., Tsukahara, S., and Tomida, A. (2017). BRAF-mutated cells activate GCN2-mediated integrated stress response as a cytoprotective mechanism in response to vemurafenib. Biochem. Biophys. Res. Commun. 482, 1491–1497.

Pakos-Zebrucka, K., Koryga, I., Mnich, K., Ljujic, M., Samali, A., and Gorman, A.M. (2016). The

integrated stress response. EMBO Rep. *17*, 1374–1395.

Park, Y., Reyna-Neyra, A., Philippe, L., and Thoreen, C.C. (2017). mTORC1 balances cellular amino acid supply with demand for protein synthesis through post-transcriptional control of ATF4. Cell Rep. *19*, 1083–1090.

Parmenter, T.J., Kleinschmidt, M., Kinross, K.M., Bond, S.T., Li, J., Kaadige, M.R., Rao, A., Sheppard, K.E., Hugo, W., Pupo, G.M., et al. (2014). Response of BRAF-mutant melanoma to BRAF inhibition is mediated by a network of transcriptional regulators of glycolysis. Cancer Discov. *4*, 423–433.

Raha, D., Wilson, T.R., Peng, J., Peterson, D., Yue, P., Evangelista, M., Wilson, C., Merchant, M., and Settleman, J. (2014). The cancer stem cell marker aldehyde dehydrogenase is required to maintain a drug-tolerant tumor cell subpopulation. Cancer Res. *74*, 3579–3590.

Richter, J.D., and Sonenberg, N. (2005). Regulation of cap-dependent translation by eIF4E inhibitory proteins. Nature *433*, 477–480.

Robert, C., Karaszewska, B., Schachter, J., Rutkowski, P., Mackiewicz, A., Stroiakovski, D., Lichinitser, M., Dummer, R., Grange, F., Mortier, L., et al. (2015). Improved overall survival in melanoma with combined dabrafenib and trametinib. New Engl. J. Med. *372*, 30–39.

Rozovsky, N., Butterworth, A.C., and Moore, M.J. (2008). Interactions between eIF4AI and its accessory factors eIF4B and eIF4H. RNA *14*, 2136–2148.

Schadendorf, D., van Akkooi, A.C.J., Berking, C., Griewank, K.G., Gutzmer, R., Hauschild, A., Stang, A., Roesch, A., and Ugurel, S. (2018). Melanoma. Lancet *392*, 971–984.

Shabaneh, T.B., Molodtsov, A.K., Steinberg, S.M., Zhang, P., Torres, G.M., Mohamed, G.A., Boni, A., Curiel, T.J., Angeles, C.V., and Turk, M.J. (2018). Oncogenic BRAF(V600E) governs regulatory T-cell recruitment during melanoma tumorigenesis. Cancer Res. *78*, 5038–5049.

Sharma, S.V., Lee, D.Y., Li, B., Quinlan, M.P., Takahashi, F., Maheswaran, S., McDermott, U., Azizian, N., Zou, L., Fischbach, M.A., et al. (2010). A chromatin-mediated reversible drug-tolerant state in cancer cell subpopulations. Cell *141*, 69–80.

Silvera, D., Formenti, S.C., and Schneider, R.J. (2010). Translational control in cancer. Nat. Rev. Cancer *10*, 254–266.

The Cancer Genome Atlas Network (2015). Genomic classification of cutaneous melanoma. Cell *161*, 1681–1696.

Van Allen, E.M., Wagle, N., Sucker, A., Treacy, D.J., Johannessen, C.M., Goetz, E.M., Place, C.S., Taylor-Weiner, A., Whittaker, S., Kryukov, G.V., et al. (2014). The genetic landscape of

clinical resistance to RAF inhibition in metastatic melanoma. Cancer Discov. *4*, 94–109.

Vattem, K.M., and Wek, R.C. (2004). Reinitiation involving upstream ORFs regulates ATF4 mRNA translation in mammalian cells. Proc. Natl. Acad. Sci. U S A *101*, 11269–11274.

Wang, L., Leite de Oliveira, R., Huijberts, S., Bosdriesz, E., Pencheva, N., Brunen, D., Bosma, A., Song, J.Y., Zevenhoven, J., Los-de Vries, G.T., et al. (2018). An acquired vulnerability of drug-resistant melanoma with therapeutic potential. Cell *173*, 1413–1425.e4.

Ye, J., Kumanova, M., Hart, L.S., Sloane, K., Zhang, H., De Panis, D.N., Bobrovnikova-Marjon, E., Diehl, J.A., Ron, D., and Koumenis, C. (2010). The GCN2-ATF4 pathway is critical for tumour cell survival and proliferation in response to nutrient deprivation. EMBO J. *29*, 2082–2096.

Zhang, C., Spevak, W., Zhang, Y., Burton, E.A., Ma, Y., Habets, G., Zhang, J., Lin, J., Ewing, T., Matusow, B., et al. (2015). RAF inhibitors that evade paradoxical MAPK pathway activation. Nature *526*, 583–586.

Zhao, E., Ding, J., Xia, Y., Liu, M., Ye, B., Choi, J.H., Yan, C., Dong, Z., Huang, S., Zha, Y., et al. (2016). KDM4C and ATF4 cooperate in transcriptional control of amino acid metabolism. Cell Rep. *14*, 506–519.

Supplemental Information

Disrupting ATF4 Expression Mechanisms

Provides an Effective Strategy

for BRAF-Targeted Melanoma Therapy

Ikuko Nagasawa, Masaru Koido, Yuri Tani, Satomi Tsukahara, Kazuhiro Kunimasa, and Akihiro Tomida
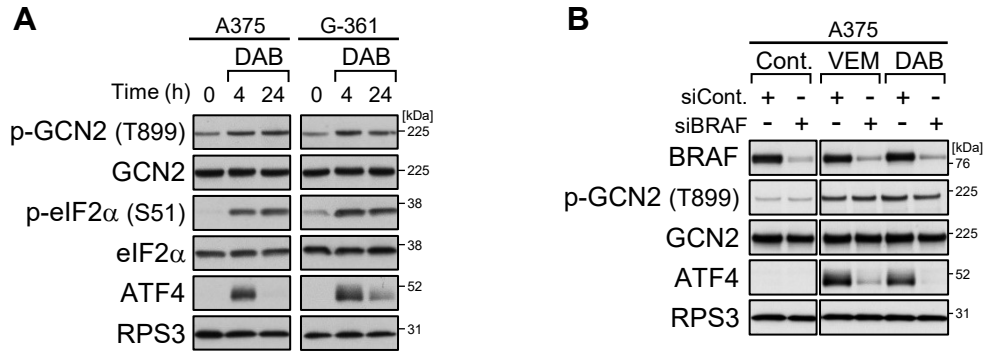
Figure S1. BRAF kinase inhibitors induce ATF4 expression transiently, related to Figure 1.

(**A**) Immunoblot analysis of A375 and G-361 cells treated with dabrafenib (DAB, 1 µM) for 4 or 24 h. (**B**) Immunoblot analysis of A375 and G-361 cells with *BRAF* knockdown by alternative siRNA (Silencer select) and treatment with vemurafenib (VEM, 10 µM) or dabrafenib (1 µM) for 4 h.
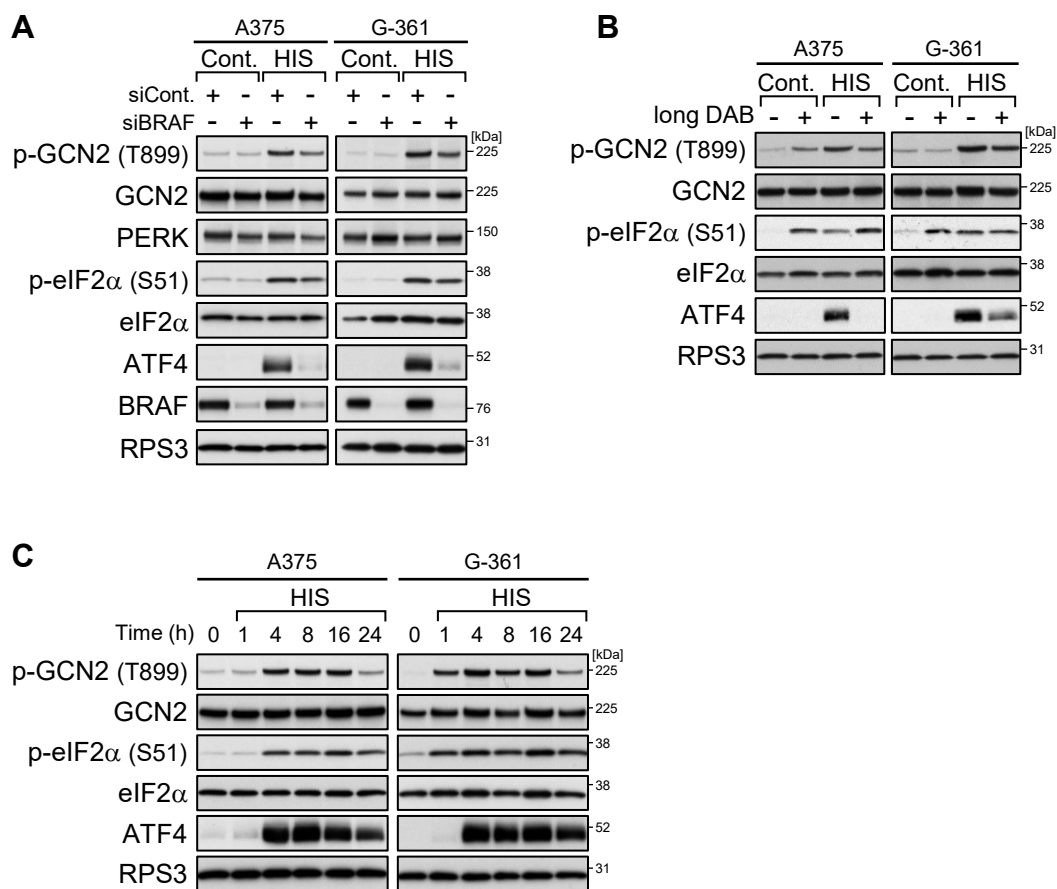
Figure S2. BRAF depletion or prolonged BRAF kinase inhibition prevents ATF4 induction, related to Figure 2.
(**A**) Immunoblot analysis of A375 and G-361 cells with *BRAF* knockdown by alternative siRNA (Silencer select) and treatment with L-histidinol (HIS, 2 mM) for 4 h. (**B**) Immunoblot analysis of A375 and G-361 cells treated with dabrafenib (DAB, 1 µM) for 24 h and then treated with L-histidinol (2 mM) for 4 h. (**C**) Immunoblot analysis of A375 and G-361 cells treated with L-histidinol (2 mM) for the indicated times.
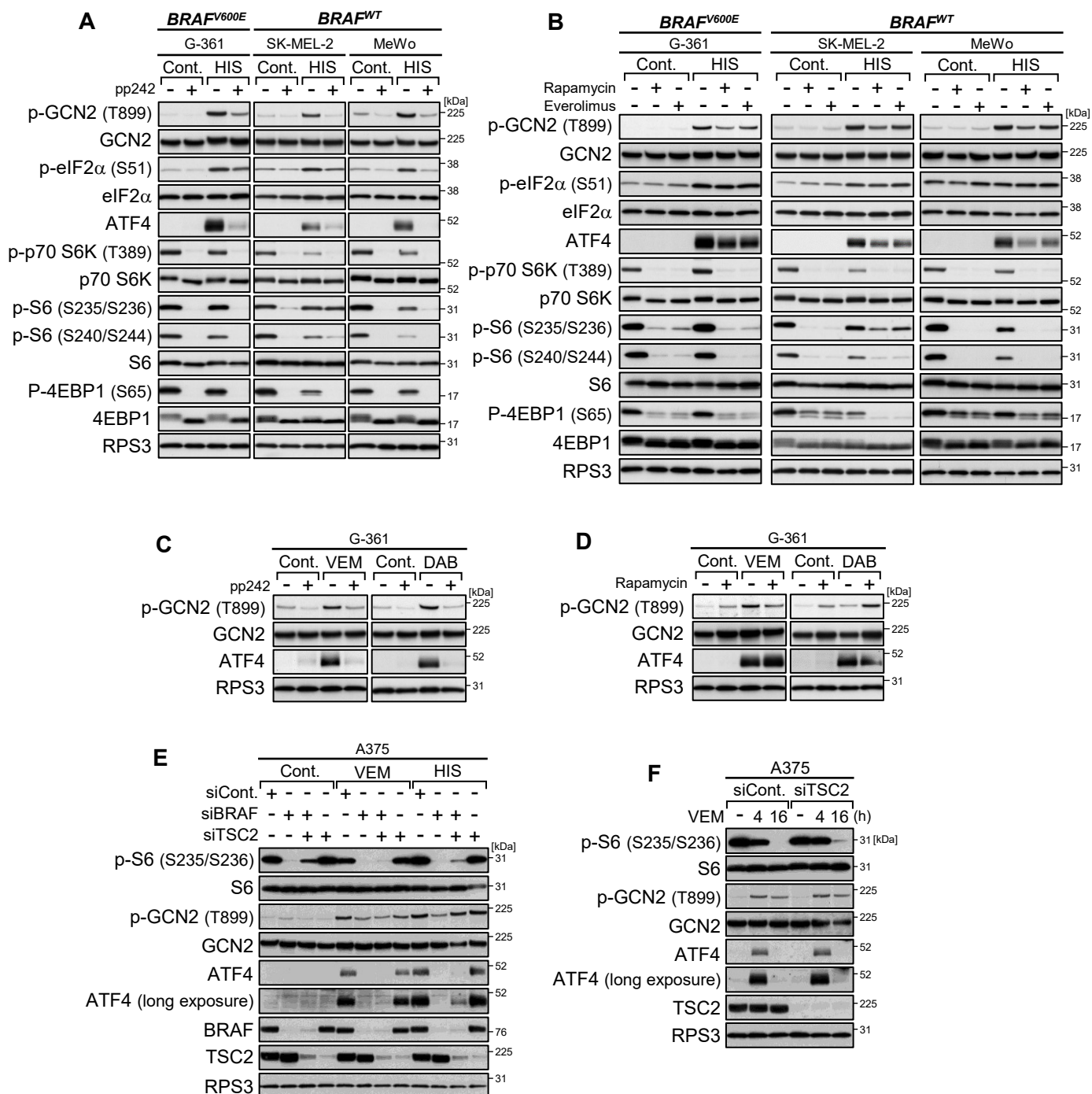
Figure S3. Oncogenic BRAF utilizes mTOR signaling pathway for ATF4 induction, related to Figure 3.

(**A**, **B**) Immunoblot analysis of the melanoma cell lines treated with L-histidinol (HIS, 2 mM) alone or in combination with pp242 (1 µM) (**A**) or with rapamycin (0.1 µM) or everolimus (0.1 µM) (**B**) for 4 h. (**C**, **D**) Immunoblot analysis of G-361 cells treated with vemurafenib (VEM, 10 µM) or dabrafenib (DAB, 1 µM) alone or in combination with pp242 (1 µM) (**C**) or with rapamycin (0.1 µM) (**D**) for 4 h. (**E**, **F**) Immunoblot analysis of A375 cells with *TSC2* knockdown by siRNA (ON-TARGETplus SMARTpool) and treatment with vemurafenib (10 µM) or L-histidinol (2 mM) for 4 h (**E**) or 16 h.
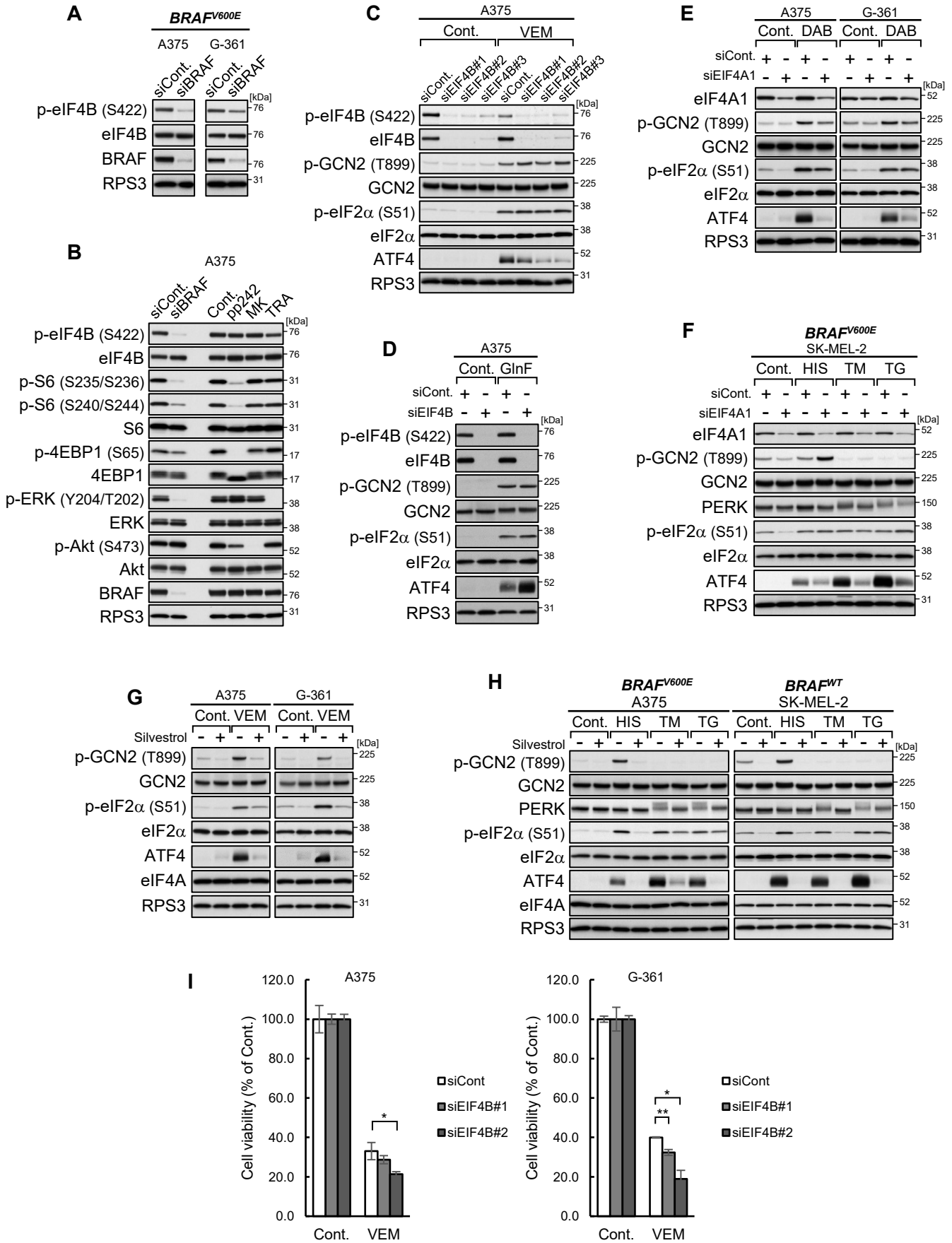
Figure S4. Oncogenic BRAF enhances eIF4B phosphorylation for ATF4 induction, related to Figure 4.

(**A**) Immunoblot analysis of A375 and G-361 cells with *BRAF* knockdown by alternative siRNA (Silencer select). (**B**) Immunoblot analysis of A375 cells with *BRAF* knockdown or treatment with pp242 (1 µM), Akt inhibitor MK-2206 (MK, 1 µM), or trametinib (TRA, 0.1 µM) for 4 h. (**C**) Immunoblot analysis of A375 cells with *EIF4B* knockdown by alternative siRNAs (Silencer select) and treatment with vemurafenib (10 µM) for 4 h. (**D**) Immunoblot analysis of A375 cells with *EIF4B* knockdown cultured in glutamine-free (GlnF) medium for 18 h. (**E**, **F**) Immunoblot analysis of the melanoma cell lines with *EIF4A1* knockdown and treatment with dabrafenib (DAB, 1 µM) (**E**) or with L-histidinol (HIS, 2 mM), tunicamycin (TM, 1 µg/ml), or thapsigargin (TG, 0.3 µM) (**F**) for 4 h. (**G**, **H**) Immunoblot analysis of the melanoma cell lines treated with silvestrol (50 nM) alone or in combination with vemurafenib (10 µM) (**G**) or L-histidinol (2 mM), tunicamycin (1 µg/ml), or thapsigargin (0.3 µM) (**H**) for 4 h. (**I**) A375 and G-361 cells were transfected with *EIF4B*-specific siRNA and treated with vemurafenib (10 µM) for 48 h. Results are shown as the mean $\pm$ SD (n=3). The p values were calculated by two-tailed *t*-test. **p < 0.01, *p < 0.05. Results are representative of two independent experiments.
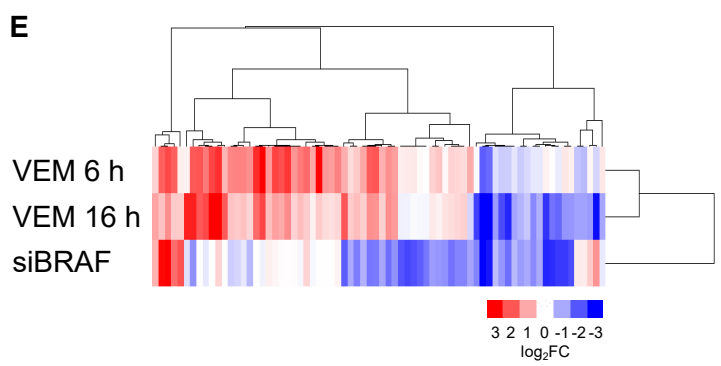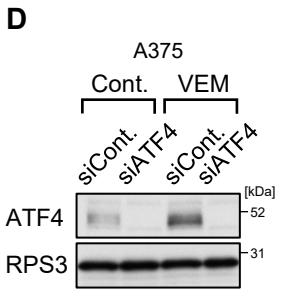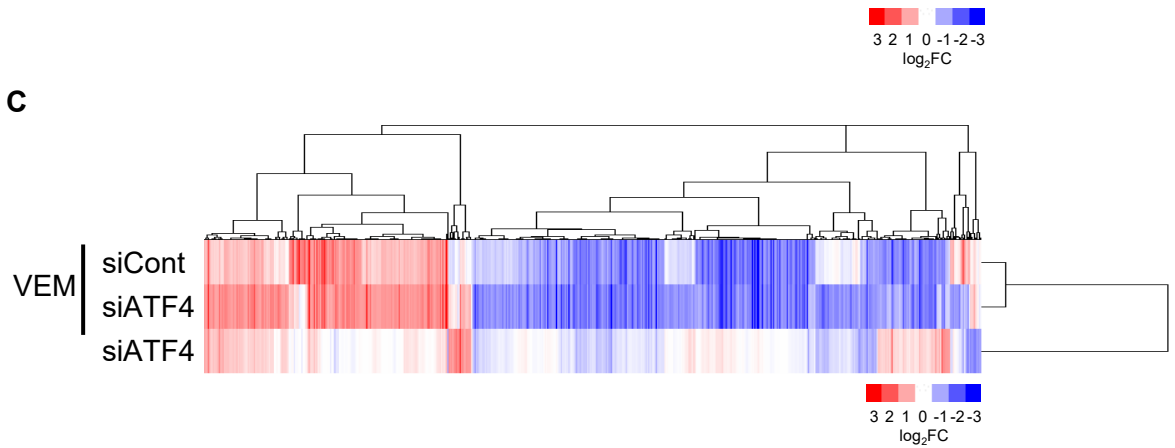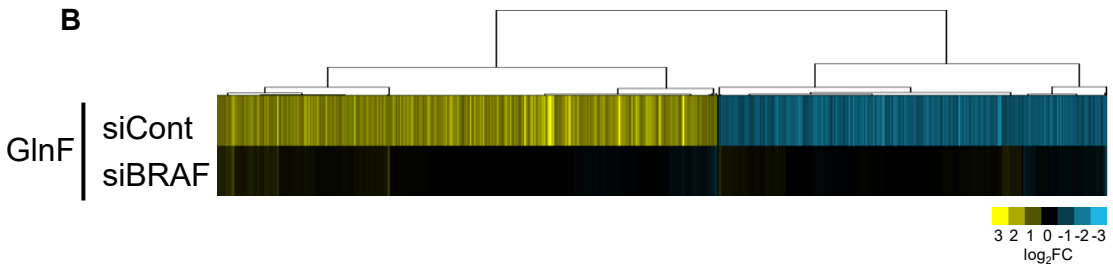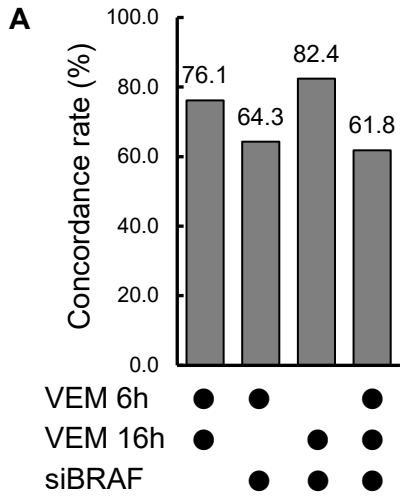
A

B

C

D

E

Figure S5. Expression of ATF4 target genes is influenced by BRAF inhibition, related to Figure 5.

(**A**) Concordance rates between the BRAF-inhibiting perturbations in Figure 5A. (**B**) Signature of 2,130 probe sets (1,574 genes) that were upregulated or downregulated under glutamine deprivation (GlnF) for 18 h in A375 cells with BRAF knockdown. The log2 fold change of levels upon glutamine deprivation is shown for each indicated knockdown condition. For probe lists, see Table S3. (**C**) Signature of 1,117 probe sets (781 genes) that were either upregulated or downregulated by treatment with vemurafenib and/or knockdown of *ATF4*. A375 cells were transfected with non-targeting siRNA (siCont) or siRNA specific for *ATF4* and then treated with vemurafenib (VEM, 10 μM) for 4 h. The log2 fold change of levels under the indicated conditions is shown for the conditions of transfection with nontargeting siRNA (siCont) and treatment with DMSO. For probe lists, see Supplementary Table S4. (**D**) Immunoblot analysis of A375 cells with *ATF4* knockdown and treatment with vemurafenib (10 μM) for 4 h. (**E**) Signature of 72 probe sets (56 genes) that overlapped between probe sets altered by BRAF-inhibiting perturbations (Figure 5A) and probe sets of the BRAFi–ATF4 signature (Figure 5B). For probe lists, see Supplementary Table S6.
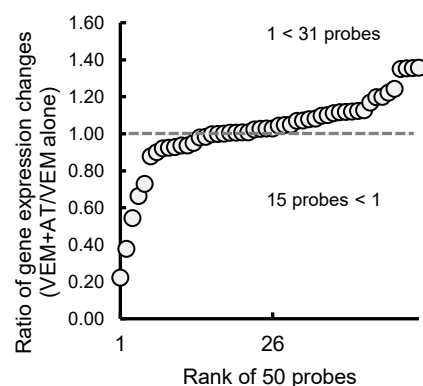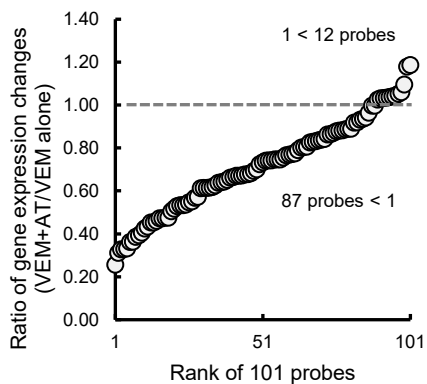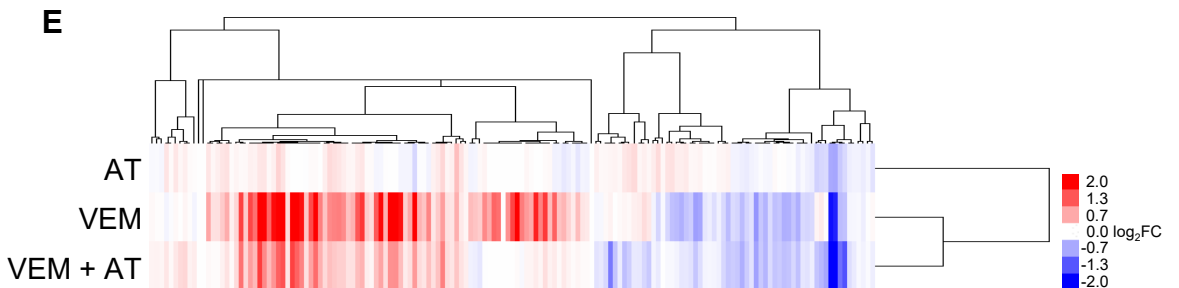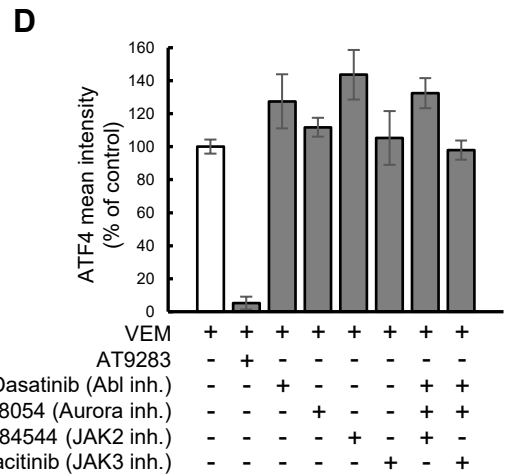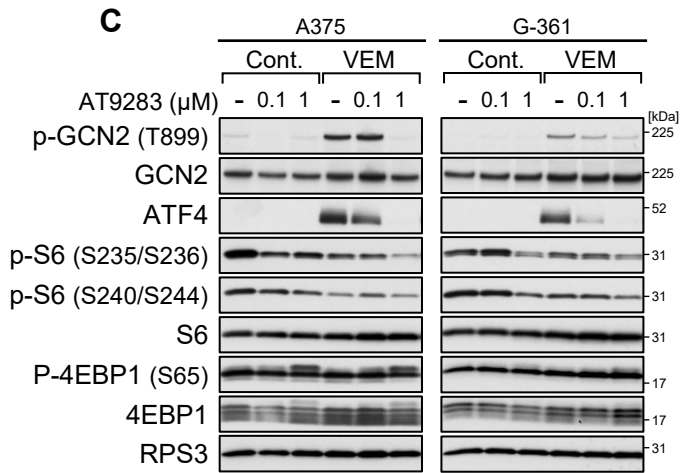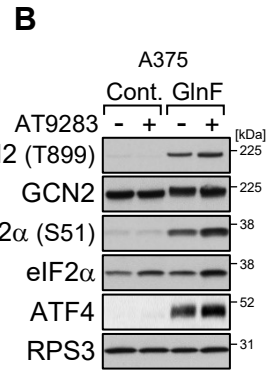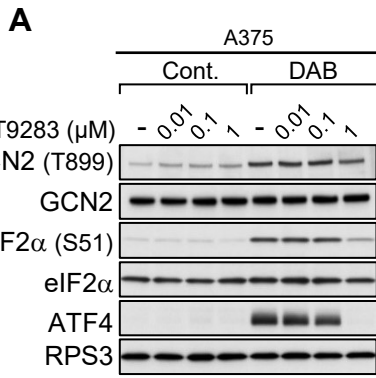
Figure S6. Identification of a chemical compound that suppresses GCN2–ATF4 pathway activation during BRAF kinase inhibition, related to Figure 6.

(**A**) Immunoblot analysis of A375 cells treated with AT9283 alone or in combination with dabrafenib (DAB, 1 µM) for 4 h. (**B**) Immunoblot analysis of A375 cells in the presence of AT9283 (1 µM) in glutamine-free (GlnF) medium for 18 h. (**C**) Immunoblot analysis of A375 and G-361 cells treated with AT9283 alone or in combination with vemurafenib (VEM, 10 µM) for 4 h. (**D**) A375 cells were treated with vemurafenib (10 µM) in the presence or absence of AT9283 (1 µM), dasatinib (1 µM), MLN8054 (1 µM), LY2784544 (1 µM), tofacitinib (1 µM), or their combinations for 6 h. The cells were fixed and stained with anti-ATF4 antibody. Bars represent the quantification of the intensity of ATF4 signals in the nucleus. Results are shown as the mean ± SD (n=3). (**E**) Signature of 155 probe sets (BRAFi–ATF4 signature) under the conditions of treatment with vemurafenib (10 µM), AT9283 (0.1 µM), or both for 6 h. The log2 fold change of levels upon treatment with vemurafenib is shown for the condition of treatment with DMSO. Plots represent the ratio of gene expression changes (cotreatment of vemurafenib with AT9283 vs. vemurafenib alone; left panel, rank of 101 probes upregulated by vemurafenib alone; right panel, rank of 50 probes downregulated by vemurafenib alone).

Scale bars, 100 μm
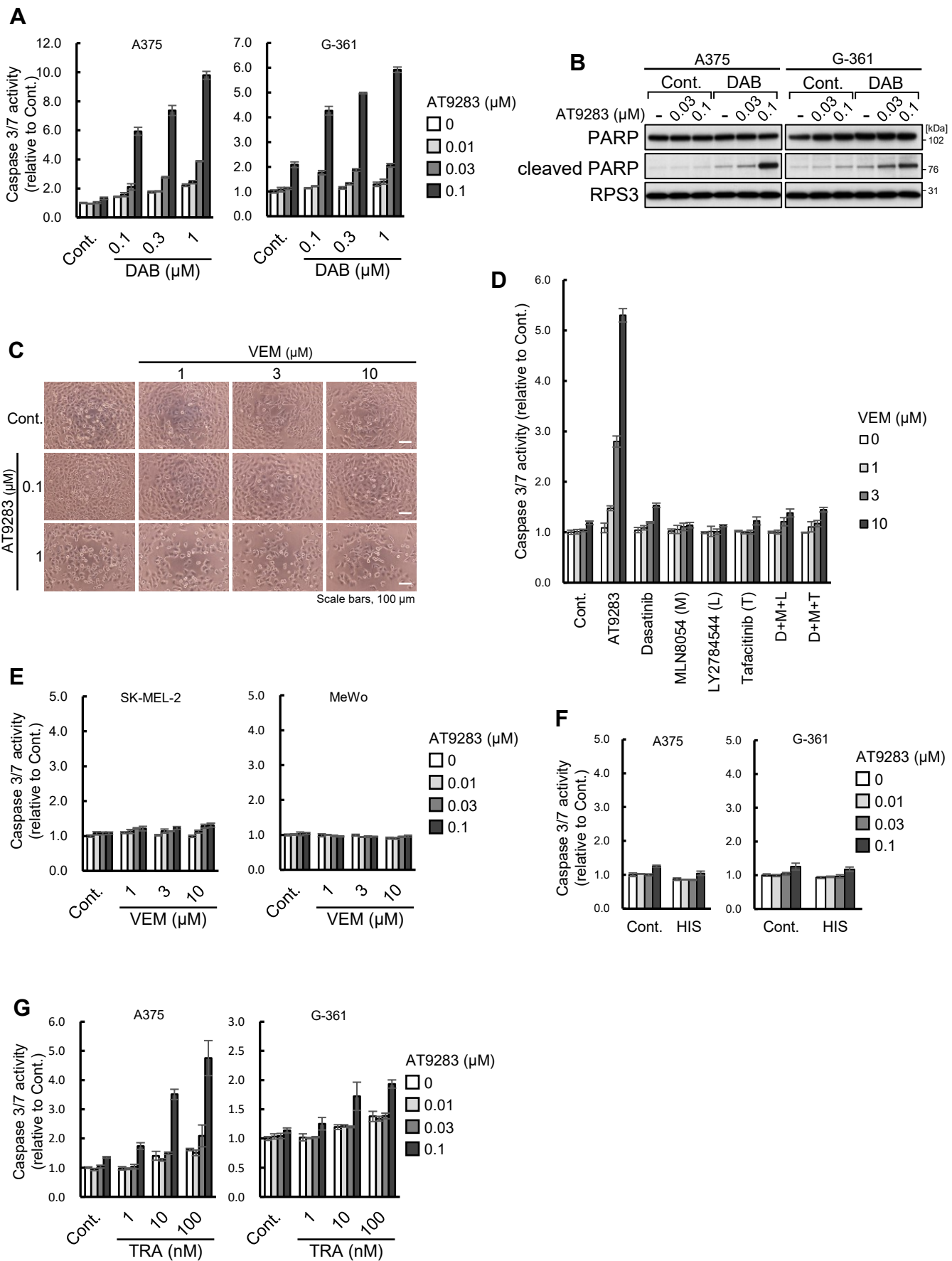
Figure S7. Enhanced growth inhibition by combined treatments with BRAF inhibitors and AT9283, related to Figure 7.

(**A**) A375 and G-361 cells were treated with AT9283 alone or in combination with dabrafenib (DAB) for 16 h. The caspase-3/7 activities were measured by the Caspase-Glo 3/7 assay. Results are shown as the mean ± SD (n=3). (**B**) Immunoblot analysis of A375 and G-361 cells treated with AT9283 alone or in combination with dabrafenib for 16 h. (**C**) Representative images of A375 cells treated with AT9283 alone or in combination with vemurafenib (VEM) for 16 h. (**D**) A375 cells were treated with vemurafenib in the presence or absence of AT9283 (0.1 µM), dasatinib (0.1 µM), MLN8054 (0.1 µM), LY2784544 (0.1 µM), tofacitinib (0.1 µM), or their combinations for 16 h. The caspase-3/7 activities were measured by the Caspase-Glo 3/7 assay. Results are shown as the mean ± SD (n=3). (**E–G**) The melanoma cell lines were treated with AT9283 alone or in combination with vemurafenib (**E**), L-histidinol (HIS, 2 mM) (**F**), or trametinib (TRA) (**G**) for 16 h. The caspase-3/7 activities were measured by the Caspase-Glo 3/7 assay. Results are shown as the mean ± SD (n=3).

TRANSPARENT METHODS

Cell lines, Reagents, and Software

Cell lines	Source	Catalog number
A375	ATCC	CRL-1619
G-361	ATCC	CRL-1424
SK-MEL-2	ATCC	HTB-68
MeWo	ATCC	HTB-65
HEK293T	ATCC	CRL-3216

Antibodies	Source	Catalog number
Rabbit monoclonal anti-phospho-eIF2α (Ser51)	Cell Signaling Technology	# 3398
Rabbit monoclonal anti-ATF4	Cell Signaling Technology	# 11815
Rabbit anti-GCN2	Cell Signaling Technology	# 3302
Rabbit monoclonal anti-phospho-p44/42 MAPK (Erk1/2) (Thr202/Tyr204)	Cell Signaling Technology	# 4370
Rabbit monoclonal anti-p44/42 MAPK (Erk1/2)	Cell Signaling Technology	# 4695
Rabbit monoclonal anti-phospho-Akt (Ser473)	Cell Signaling Technology	# 4060
Rabbit monoclonal anti-Akt (pan)	Cell Signaling Technology	# 4685
Rabbit monoclonal anti-phospho-p70 S6 Kinase (Thr389)	Cell Signaling Technology	# 9234
Rabbit anti-p70 S6 Kinase	Cell Signaling Technology	# 9202
Rabbit anti-phospho-S6 Ribosormal Protein (Ser235/236)	Cell Signaling Technology	# 2211
Rabbit anti-phospho-S6 Ribosormal Protein (Ser240/244)	Cell Signaling Technology	# 2215
Rabbit monoclonal anti-S6 Ribosormal Protein	Cell Signaling Technology	# 2217
Rabbit monoclonal anti-TSC2	Cell Signaling Technology	#4308
Rabbit monoclonal anti-phospho-4E-BP1 (Ser65)	Cell Signaling Technology	# 9456

Rabbit monoclonal anti-phospho-4E-BP1	Cell Signaling Technology	# 9644
Rabbit anti-phospho-eIF4B (Ser422)	Cell Signaling Technology	# 3591
Rabbit anti-eIF4B	Cell Signaling Technology	# 3592
Rabbit anti-eIF4A1	Cell Signaling Technology	# 2490
Rabbit monoclonal anti-cleaved PARP (Asp214)	Cell Signaling Technology	# 5625
Rabbit monoclonal anti-PARP	Cell Signaling Technology	# 9532
Rabbit monoclonal anti-phospho-Stat3 (Tyr705)	Cell Signaling Technology	# 9145
Rabbit anti-Stat3	Cell Signaling Technology	# 9132
Rabbit anti-Ribosomal Protein L7a	Cell Signaling Technology	# 2403
Rabbit monoclonal anti-Ribosomal Protein S3	Cell Signaling Technology	# 9538
Rabbit monoclonal anti-phospho-GCN2 (Thr899)	Abcam	ab75836
Rabbit anti-PERK	Abcam	ab65142
Mouse monoclonal anti-EIF2S1	Abcam	ab5369
Mouse monoclonal anti-Raf-B	Santa Cruz Biotechnology	sc-55522
Mouse monoclonal anti-B-Raf (V600E)	NewEast Biosciences	# 26039
Mouse monoclonal anti-FLAG	Sigma-Aldrich	F3165
Goat anti-Rabbit IgG (H+L) Secondary Antibody, Alexa Fluor 488 conjugate	Thermo Fisher Scientific	A-11034

Chemicals	Source	Catalog number
Vemurafenib	Selleckchem	S1267
Dabrafenib	Selleckchem	S2807
Trametinib	Selleckchem	S2673
AT9283	Selleckchem	S1134
Dasatinib	Selleckchem	S1021
MLN8054	Selleckchem	S1100
LY2784544	Selleckchem	S2179
Tofacitinib	Selleckchem	Kinase Inhibitor Library
MK-2206	Selleckchem	S1078

Kinase Inhibitor Library	Selleckchem	Z88022
PP242	Sigma-Aldrich	N/A
Rapamycin	Sigma-Aldrich	N/A
Everolimus	Sigma-Aldrich	N/A
L-Histidinol dihydrochloride	Sigma-Aldrich	H6647
Thapsigargin	FUJIFILM Wako	205-17283
Tunicamycin	Nacalai Tesque	35638-74
Silvestrol	ChemScene	CS-0543

siRNAs	Source	Catalog number
ON-TARGETplus SMARTpool BRAF siRNA	Dharmacon	L-003460-00
ON-TARGETplus SMARTpool EIF4B siRNA	Dharmacon	L-020179-00
ON-TARGETplus SMARTpool EIF4A1 siRNA	Dharmacon	L-020178-00
ON-TARGETplus SMARTpool ATF4 siRNA	Dharmacon	L-005125-00
ON-TARGETplus SMARTpool TSC2 siRNA	Dharmacon	L-003029-00
Silencer Select BRAF siRNA	Thermo Fisher Scientific	s2080
Silencer Select EIF4B siRNA #1	Thermo Fisher Scientific	s4573
Silencer Select EIF4B siRNA #2	Thermo Fisher Scientific	s4574
Silencer Select EIF4B siRNA #3	Thermo Fisher Scientific	s4575

Plasmid	Source	Catalog number
pFLAG-B-Raf	Addgene	40775

Software	Reference	
Cluster 3.0	de Hoon et al., 2004	http://bonsai.hgc.jp/~mdehoon/software/cluster/software.htm
DAVID (version 6.8)	Huang da et al., 2009a; Huang da et al., 2009b	https://david.ncifcrf.gov/

Enrichr	Chen et al., 2013; Kuleshov et al., 2016	https://amp.pharm.mssm.edu/Enrichr/
GSEA software (version 2.0.14)	Mootha et al., 2003; Subramanian et al., 2005	http://software.broadinstitute.org/gsea/index.jsp
Java TreeView (version 1.1.6r4)	Saldanha, 2004	http://jtreeview.sourceforge.net/
R (version 3.3.1)	N/A	https://www.r-project.org/
RMAExpress (version 1.0.5)	Irizarry et al., 2003	http://rmaexpress.bmbolstad.com/

Cell culture

The melanoma cell lines and HEK293T cells were maintained in RPMI1640 (FUJIFILM Wako, Osaka, Japan) supplemented with 10% fetal bovine serum and 100 μg/ml kanamycin. For the glutamine withdrawal, cells were cultured in glutamine-free RPMI1640 (FUJIFILM Wako) supplemented with 10% fetal bovine serum and 100 μg/ml kanamycin.

Immunoblot analysis

Immunoblot analysis was performed as described previously (Saito et al., 2009). Briefly, cell lysates were prepared using SDS lysis buffer (62.5 mM Tris-HCl pH6.8, 2% SDS, 10% glycerol, and 50 mM DTT) and protein concentrations were determined using the Bio-Rad protein assay (Bio-Rad, Hercules, CA, USA). Protein samples were subjected to SDS-PAGE and subsequently transferred onto a nitrocellulose membrane. The specific bands were detected using Western Lightning plus ECL (Perkin Elmer, Waltham, MA, USA).

RNA interference

Silencing of human *BRAF*, *TSC2*, *EIF4B*, *EIF4A1*, and *ATF4* expression was performed using ON-TARGETplus SMARTpool siRNA (Dharmacon, Lafayette, CO, USA) or Silencer Select siRNA (Thermo Fisher Scientific, Waltham, MA, USA) with Lipofectamine RNAiMAX (Thermo Fisher Scientific). ON-TARGETplus SMARTpool and Silencer Select siRNAs were used at 20 and 5 nM, respectively. Cells were transfected with each siRNA, in accordance with the manufacturer's reverse-transfection protocol.

Overexpression of BRAF

For BRAF V600E point mutation in the FLAG-BRAF expression vector, site-directed mutagenesis was carried out using a QuickChange Mutagenesis Kit (Agilent Technologies, Santa Clara, CA, USA). Transient transfections into HEK293T and A375 cells were performed using Lipofectamine 2000 (Thermo Fisher Scientific).

Cell viability assay

Cells were transfected with *EIF4B*-specific siRNA and cultured at 1×10^3 (A375) or 2×10^3 (G-361) cells/well in a 96-well plate. After 24 h, the cells were treated with vemurafenib for 48 h. For cell regrowth assay, the cells were seeded at 5×10^3 (A375) or 1×10^4 (G-361) cells/well in a 96-well plate and treated with AT9283, vemurafenib, or both for 16 h. The cells were reseeded to a new 96-well plate and cultured in drug-free medium for 96 h. Cell viability was determined by the CellTiter-Glo luminescent cell viability assay (Promega, Madison, WI, USA) based on quantification of the ATP content.

Chemical screening

A375 cells were seeded at 8×10^3 cells/well in a 96-well plate and treated with each compound (2 μM) from the Kinase Inhibitor Library (355 kinase inhibitors, Selleck) in combination with vemurafenib (10 μM) for 6 h. The cells were fixed and subjected to fluorescent immunostaining using anti-ATF4 antibody as described below.

Fluorescent immunostaining

A375 cells (8×10^3 cells/well in a 96-well plate) were treated with vemurafenib, L-histidinol, or tunicamycin in the presence or absence of kinase inhibitors for 6 h. For comparison of the effects of AT9283, dasatinib, MLN8054, LY2784544, and tofacitinib, cells were treated with each compound at 1 μM, a concentration enough to inhibit each target kinase activity, based on the previous reports (Flanagan et al., 2010; Howard et al., 2009; Ma et al., 2013; Manfredi et al., 2007; O'Hare et al., 2005). The cells were subjected to fluorescent immunostaining using anti-ATF4 antibody, as described previously (Nagasawa et al., 2017). Fluorescent images were acquired by IN Cell Analyzer 6000 (GE Healthcare, Chicago, IL, USA). Quantification of ATF4 intensity in the nucleus was performed using IN Cell Developer Toolbox software (GE Healthcare).

Caspase-3/7 activity assay

Cells were seeded at 5×10^3 (A375) or 1×10^4 (G-361) cells/well in a 96-well plate and treated with vemurafenib, L-histidinol, or trametinib in the presence or absence of AT9283, dasatinib, MLN8054, LY2784544, tofacitinib, or their combinations for 16 h. The caspase-3/7 activities were measured by the Caspase-Glo 3/7 assay (Promega).

Colony formation assay

A375 and G-361 cells were treated with AT9283, vemurafenib, or both for 16 h, and then reseeded in six-well plates (A375: 1×10^3 cells/well, G361: 2×10^3 cells/well). After 7 (A375) or 14 (G-361) days, the colonies were stained with crystal violet.

Microarray

Microarray analysis was carried out as described previously (Saito et al., 2009). The data were normalized by the Robust Multichip Average method using RMAExpress 1.0.5 (Irizarry et al., 2003). Probes with a signal intensity value of < 50 were treated as having a fixed value of 50 (Mashima et al., 2015). Signatures of gene sets were selected using the signal intensity ratio relative to each control sample as follows: probes with fold change > 1.5 (< 0.75) are upregulated (downregulated) ones in Figure 6E; probe with fold change > 2 (< 0.5) are upregulated (downregulated) ones for other signatures. Control samples are described in each figure legend. Clustering analysis was performed using the correlation-based distance and complete linkage method by Cluster 3.0 software (de Hoon et al., 2004) and visualized by Java TreeView (Saldanha, 2004). Gene Ontology analysis was performed using DAVID (National Institute of Allergy and Infectious Diseases, NIH, MD, USA) with the default parameters (Huang da et al., 2009a, b) and Enrichr (Chen et al., 2013; Kuleshov et al., 2016).

TCGA analysis

Preprocessed RNA-sequenced transcriptome data and BRAF mutation status of skin cutaneous melanoma (SKCM; 472 donors), including primary and metastasis tumors, were obtained from The Cancer Genome Atlas (TCGA) (Broad Institute TCGA Genome

Data Analysis Center (2016): Firehose stddata_2016_01_28 run; Broad Institute of MIT and Harvard; doi:10.7908/C11G0KM9) (2015) via the cBioPortal (Cerami et al., 2012; Gao et al., 2013) website (downloaded on 3/26/2017). For log2-scaled expression levels of each gene, we calculated the regression coefficients of BRAF V600* mutation status including V600E, V600G, V600M, V600V, and V600_K601delinsE (166 donors) by regressing out the covariate of NRAS or NF1 mutation status (138 donors), which are mutually exclusive with BRAF mutations. We established rankings of genes in descending order of the fitted coefficients for prerank mode of GSEA analysis with 1×10^4 permutations (Mootha et al., 2003; Subramanian et al., 2005). From the BRAFi–ATF4 signature, we excluded *ATF4* and genes that were not included in the TCGA transcriptome data set and tested the enrichment of the remaining 107 genes. For such processing, we used the statistical computing language R (https://www.r-project.org/; version 3.3.1).

Data and Software Availability

The accession number for the microarray data reported in this paper is National Center for Biotechnology Information Gene Expression Omnibus: GSE136615.

Statistics

Data are presented as mean ± S.D. from at least three independent experiments.

SUPPLEMENTAL REFERENCES

Cerami, E., Gao, J., Dogrusoz, U., Gross, B.E., Sumer, S.O., Aksoy, B.A., Jacobsen, A., Byrne, C.J., Heuer, M.L., Larsson, E*., et al.* (2012). The cBio cancer genomics portal: an open platform for exploring multidimensional cancer genomics data. Cancer Discov *2*, 401-404.

Chen, E.Y., Tan, C.M., Kou, Y., Duan, Q., Wang, Z., Meirelles, G.V., Clark, N.R., and Ma'ayan, A. (2013). Enrichr: interactive and collaborative HTML5 gene list enrichment analysis tool. BMC bioinformatics *14*, 128.

de Hoon, M.J., Imoto, S., Nolan, J., and Miyano, S. (2004). Open source clustering software. Bioinformatics (Oxford, England) *20*, 1453-1454.

Flanagan, M.E., Blumenkopf, T.A., Brissette, W.H., Brown, M.F., Casavant, J.M., Shang-Poa, C., Doty, J.L., Elliott, E.A., Fisher, M.B., Hines, M*., et al.* (2010). Discovery of CP-690,550: a potent and selective Janus kinase (JAK) inhibitor for the treatment of autoimmune diseases and organ transplant rejection. Journal of medicinal chemistry *53*, 8468-8484.

Gao, J., Aksoy, B.A., Dogrusoz, U., Dresdner, G., Gross, B., Sumer, S.O., Sun, Y., Jacobsen, A., Sinha, R., Larsson, E*., et al.* (2013). Integrative analysis of complex cancer genomics and clinical profiles using the cBioPortal. Science signaling *6*, pl1.

Huang da, W., Sherman, B.T., and Lempicki, R.A. (2009a). Bioinformatics enrichment tools: paths toward the comprehensive functional analysis of large gene lists. Nucleic acids research *37*, 1-13.

Huang da, W., Sherman, B.T., and Lempicki, R.A. (2009b). Systematic and integrative analysis of large gene lists using DAVID bioinformatics resources. Nature protocols *4*, 44-57.

Irizarry, R.A., Hobbs, B., Collin, F., Beazer-Barclay, Y.D., Antonellis, K.J., Scherf, U., and Speed, T.P. (2003). Exploration, normalization, and summaries of high density oligonucleotide array probe level data. Biostatistics (Oxford, England) *4*, 249-264.

Kuleshov, M.V., Jones, M.R., Rouillard, A.D., Fernandez, N.F., Duan, Q., Wang, Z., Koplev, S., Jenkins, S.L., Jagodnik, K.M., Lachmann, A*., et al.* (2016). Enrichr: a comprehensive gene set enrichment analysis web server 2016 update. Nucleic acids research *44*, W90-97.

Ma, L., Clayton, J.R., Walgren, R.A., Zhao, B., Evans, R.J., Smith, M.C., Heinz-Taheny, K.M., Kreklau, E.L., Bloem, L., Pitou, C*., et al.* (2013). Discovery and characterization of LY2784544, a small-molecule tyrosine kinase inhibitor of JAK2V617F. Blood cancer journal *3*, e109.

Manfredi, M.G., Ecsedy, J.A., Meetze, K.A., Balani, S.K., Burenkova, O., Chen, W.,

Galvin, K.M., Hoar, K.M., Huck, J.J., LeRoy, P.J*., et al.* (2007). Antitumor activity of MLN8054, an orally active small-molecule inhibitor of Aurora A kinase. Proceedings of the National Academy of Sciences of the United States of America *104*, 4106-4111.

Mashima, T., Ushijima, M., Matsuura, M., Tsukahara, S., Kunimasa, K., Furuno, A., Saito, S., Kitamura, M., Soma-Nagae, T., Seimiya, H*., et al.* (2015). Comprehensive transcriptomic analysis of molecularly targeted drugs in cancer for target pathway evaluation. Cancer science *106*, 909-920.

Mootha, V.K., Lindgren, C.M., Eriksson, K.F., Subramanian, A., Sihag, S., Lehar, J., Puigserver, P., Carlsson, E., Ridderstrale, M., Laurila, E*., et al.* (2003). PGC-1alpha-responsive genes involved in oxidative phosphorylation are coordinately downregulated in human diabetes. Nature genetics *34*, 267-273.

O'Hare, T., Walters, D.K., Stoffregen, E.P., Jia, T., Manley, P.W., Mestan, J., Cowan-Jacob, S.W., Lee, F.Y., Heinrich, M.C., Deininger, M.W*., et al.* (2005). In vitro activity of Bcr-Abl inhibitors AMN107 and BMS-354825 against clinically relevant imatinib-resistant Abl kinase domain mutants. Cancer research *65*, 4500-4505.

Saito, S., Furuno, A., Sakurai, J., Sakamoto, A., Park, H.R., Shin-Ya, K., Tsuruo, T., and Tomida, A. (2009). Chemical genomics identifies the unfolded protein response as a target for selective cancer cell killing during glucose deprivation. Cancer research *69*, 4225-4234.

Saldanha, A.J. (2004). Java Treeview--extensible visualization of microarray data. Bioinformatics (Oxford, England) *20*, 3246-3248.

Subramanian, A., Tamayo, P., Mootha, V.K., Mukherjee, S., Ebert, B.L., Gillette, M.A., Paulovich, A., Pomeroy, S.L., Golub, T.R., Lander, E.S*., et al.* (2005). Gene set enrichment analysis: a knowledge-based approach for interpreting genome-wide expression profiles. Proceedings of the National Academy of Sciences of the United States of America *102*, 15545-15550.